Нейтронное спин-эхо и квазиклассическая динамика наносистем

Лебедев В.Т.
ПИЯФ НИЦ КИ

Precession of Neutron Beam Polarization in Magnetic Field
1969, G.M.Drabkin → *Polarized beams* at PNPI

1972, Budapest, **F.Mezei**, → IN 11, ILL
Creation of NSE-spectroscopy **1972** → **1982**
Various Modifications → Resonance NSE, SESANS, NSE + TAS, TOF ….

43 Years – a critical age …

NSE – facilities ?

IN11 (Institut Laue-Langevin,ILL, Grenoble, France)
IN15 (Institut Laue-Langevin,ILL, Grenoble, France)
J-NSE (Juelich Centre for Neutron Science JCNS, Juelich, Germany, hosted by FRMII, Munich (Garching), Germany)
NG5-NSE (NIST CNRF, Gaithersburg, USA)
NSE@SNS (JCNS SNS, Oak Ridge)
RESEDA (FRM II Munich FRMII, Munich, Germany
V5/SPAN (Hahn-Meitner Institut, Berlin, Germany)
C2-2 (ISSP, Tokai, Japan)

PIK → Modern NSE Concept ?

To overcome some limitations

Wide spectrum?
Inelastic Scattering Spectroscopy + 3D polarization analysis ?
Energy transfer : Symmetry? Full spectrum = odd + even

In NSE*, Neutron Spins Precess Before and After Scattering & a Polarization Echo is Obtained if Scattering is Elastic

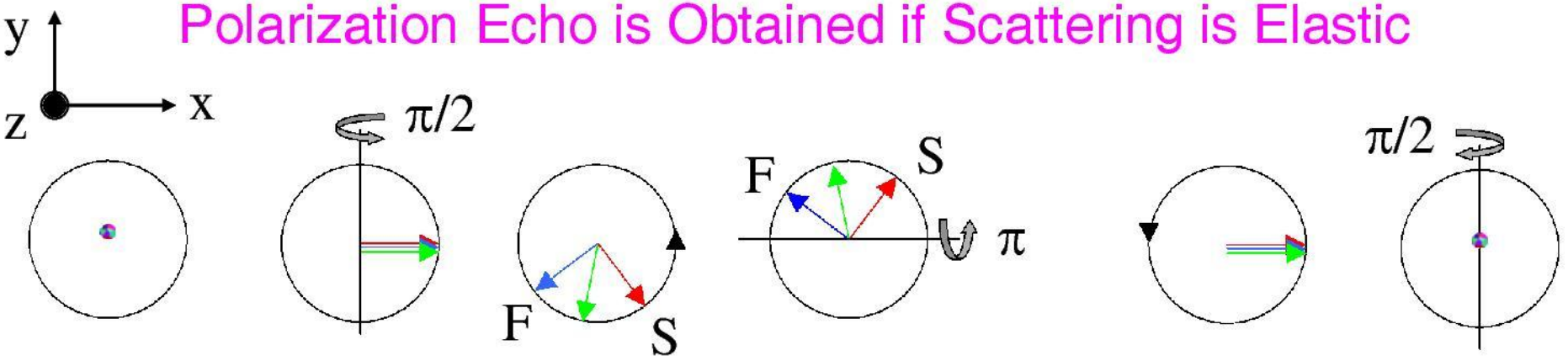

Initially, neutrons are polarized along z

Rotate spins into x-y precession plane

Allow spins to precess around z: slower neutrons precess further over a fixed path-length

Rotate spins through π about x axis

Elastic Scattering Event

Allow spins to precess around z: all spins are in the same direction at the echo point if ΔE = 0

Rotate spins to z and measure polarization

$$\textit{Final Polarization}, P = \left\langle \cos(\phi_1 - \phi_2) \right\rangle$$

* F. Mezei, Z. Physik, 255 (1972) 145

What does a NSE Spectrometer Look Like? IN11 at ILL was the First

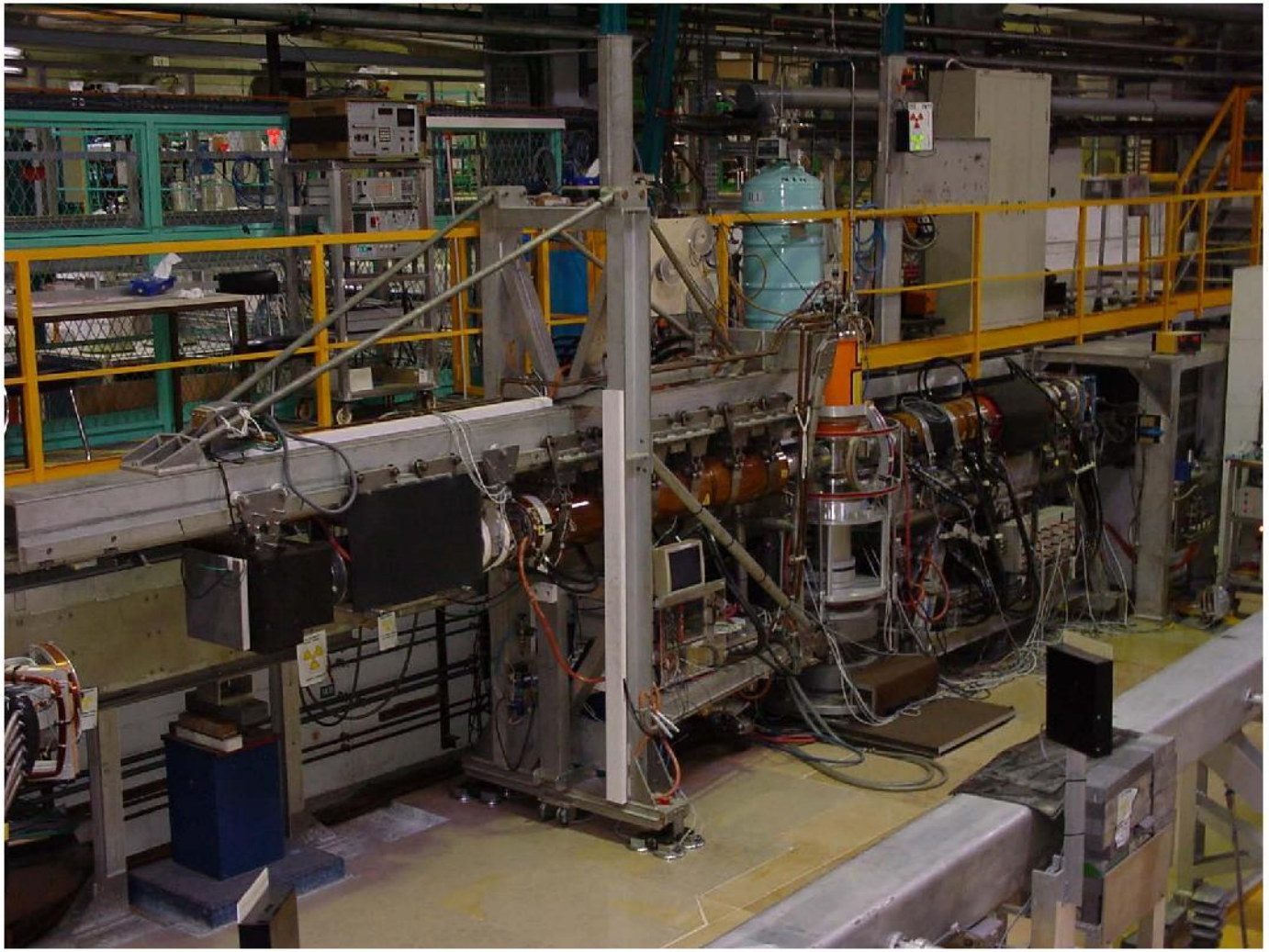

$\tau_{max} \sim 50$ ns at $\lambda = 10$ Å

IN-11C and IN15

τ_{max} ~ 12 ns at λ = 10Å for IN11-C and τ_{max} ~ 400 ns at λ = 15Å

NSE is also available at the NCNR

NIST

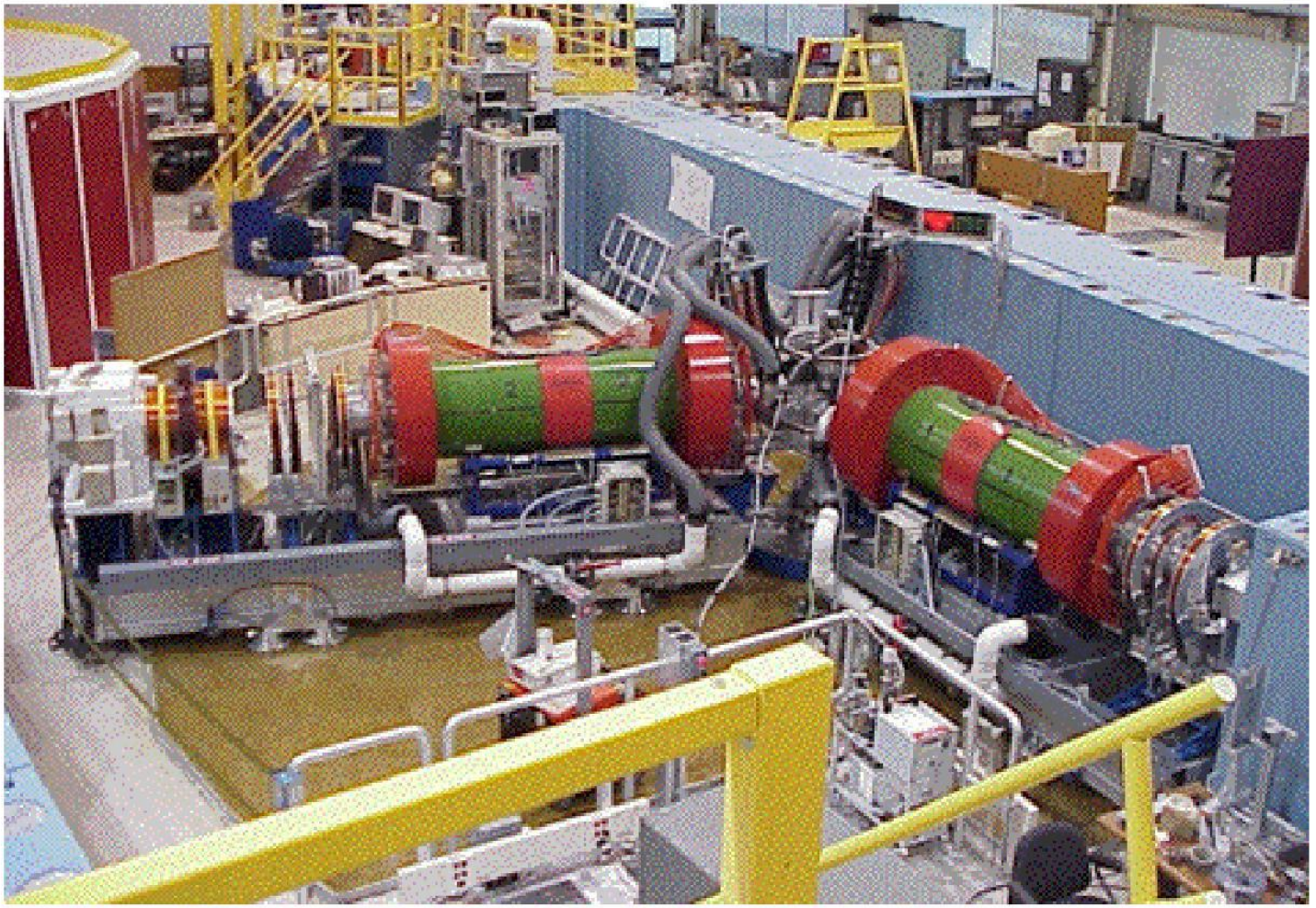

$\tau_{max} \sim 50$ ns

An NRSE Triple Axis Spectrometer at HMI: Note the Tilted Coils

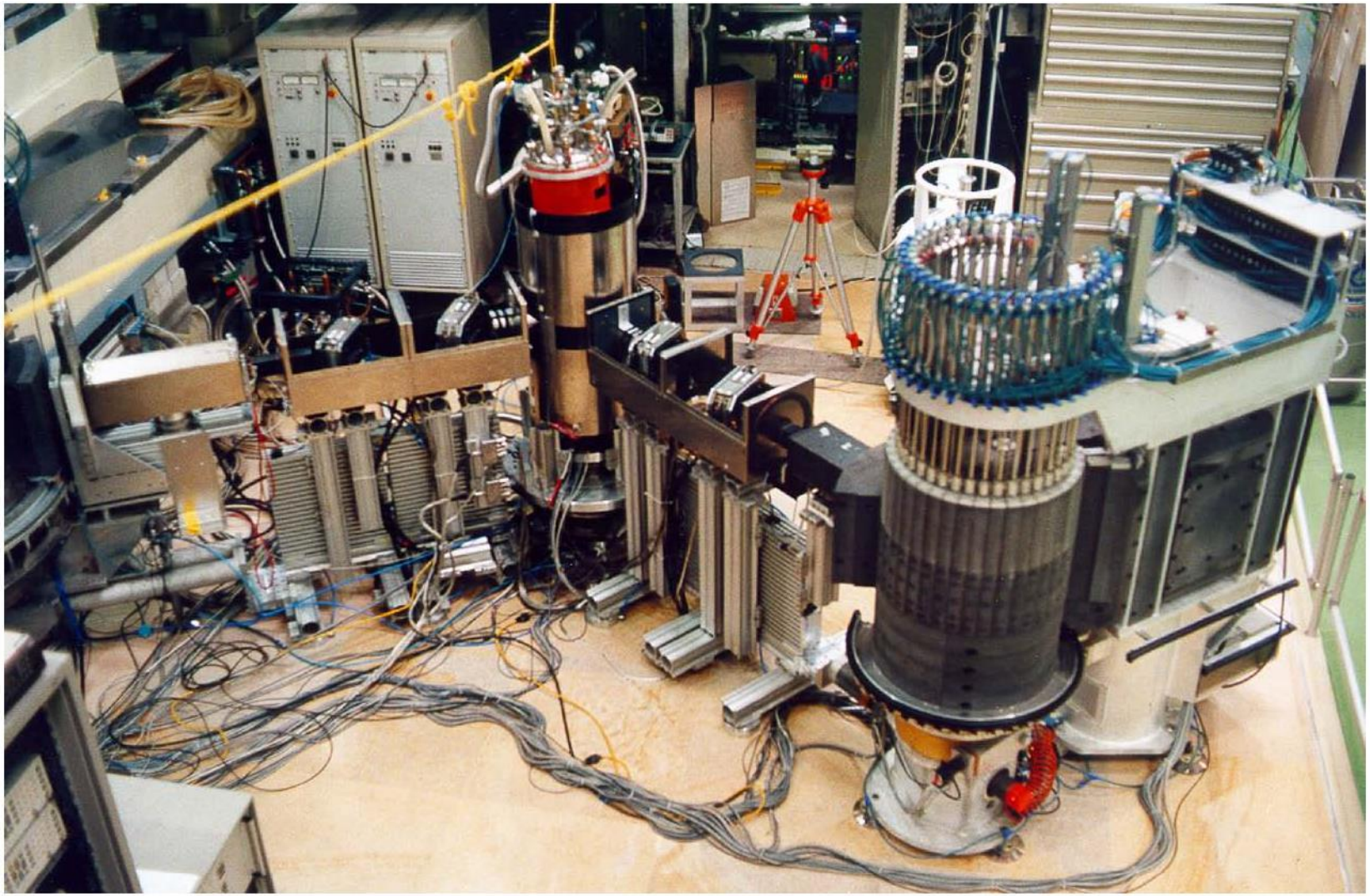

LLB, MUSES

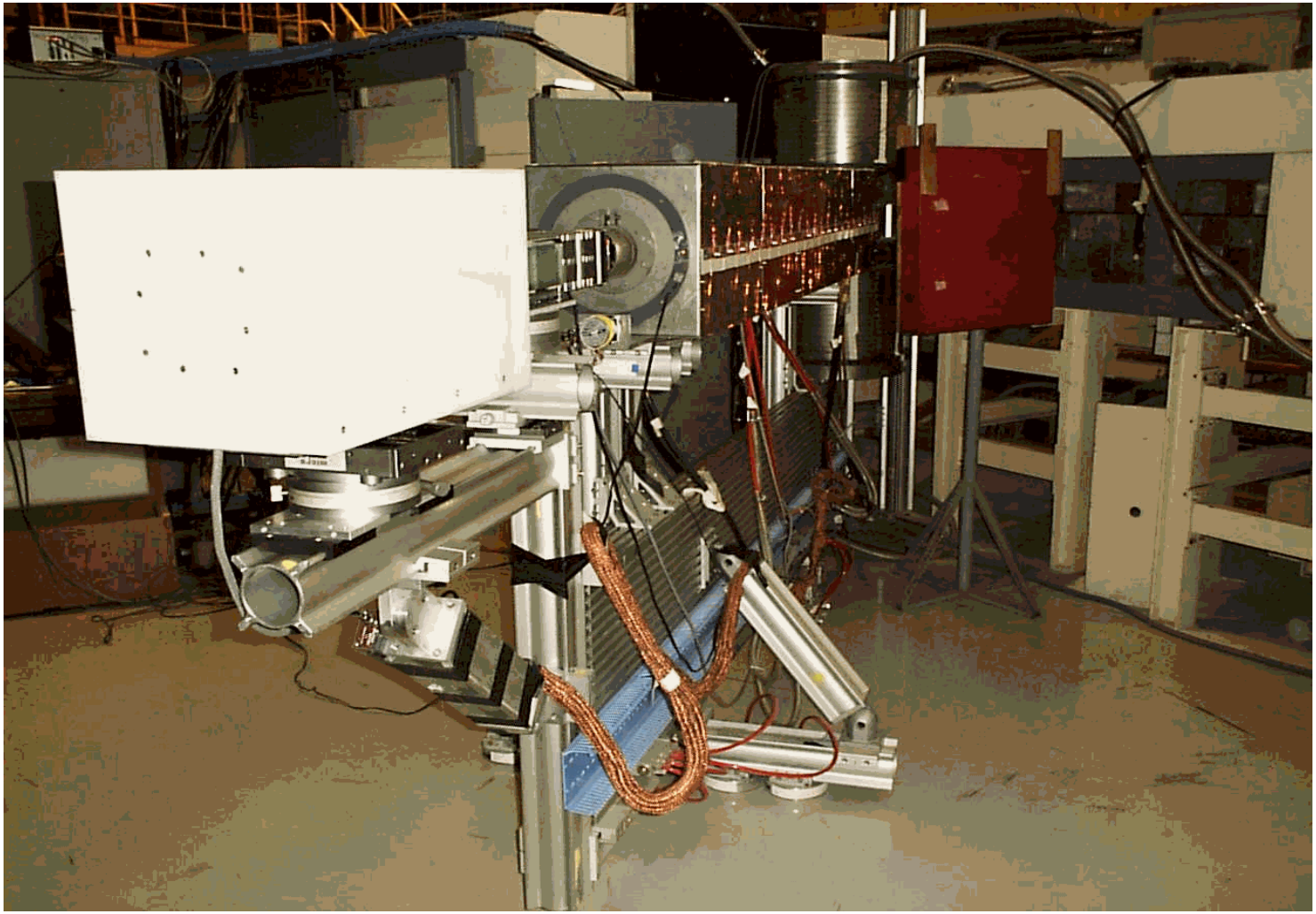

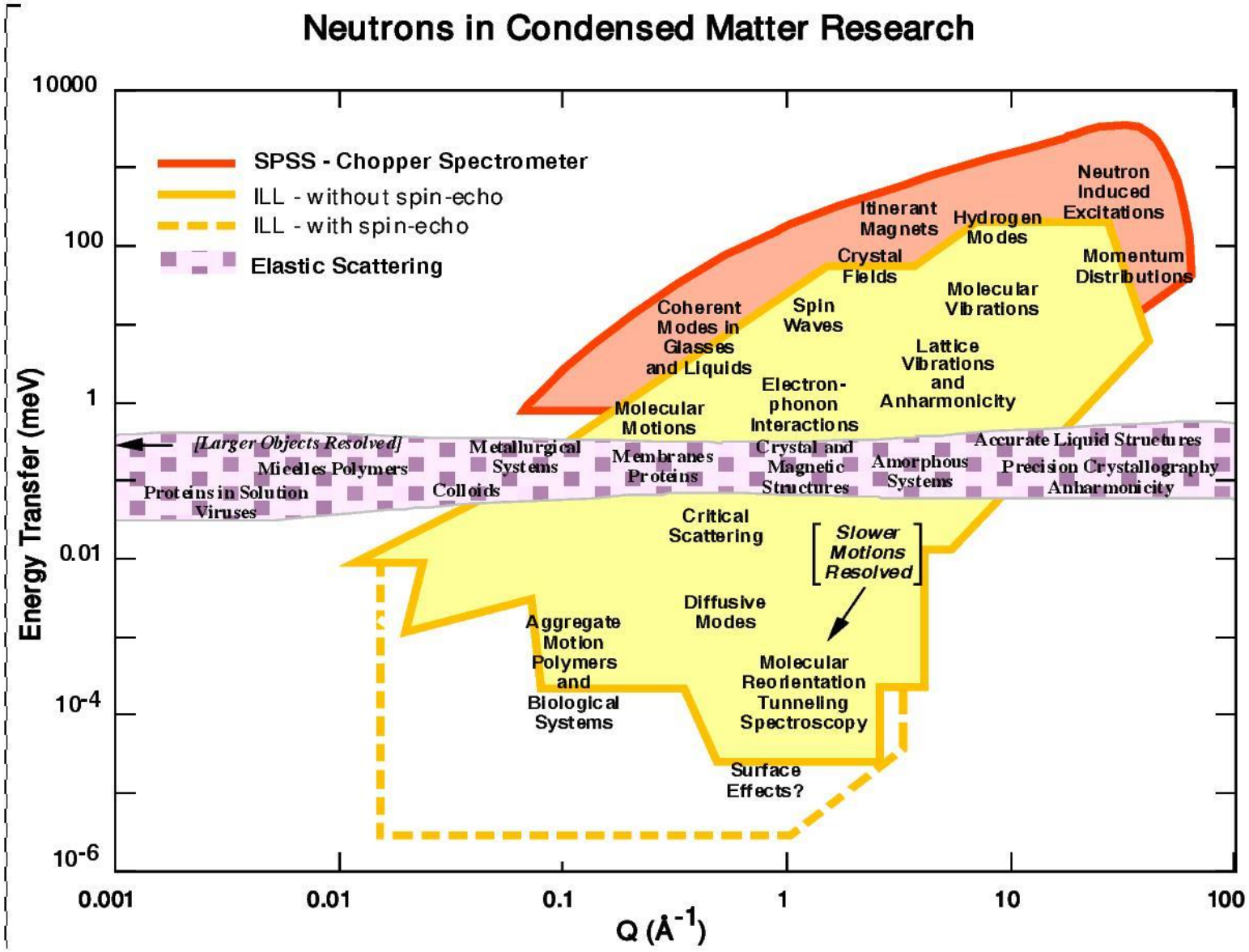

Neutron Spin Echo has significantly extended the (Q,E) range to which neutron scattering can be applied

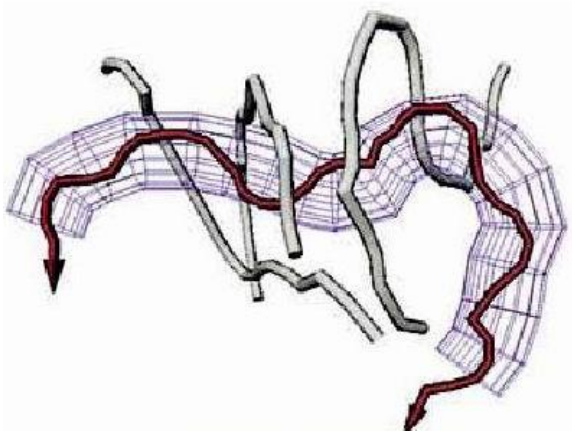

Polymer Chain Reptation

Deuterated chain in the tube of surrounding chains
Stretched segmental dynamics: $\Gamma = 1/\tau \sim q^4$
Long scale: reptation, $S(q,t) \sim \exp[-(\Gamma t)^{1/4}]$

Rouse model for segmental dynamics, slow diffusion of segments in chain: $\Delta r^2 \sim l^2 \cdot t^{1/2}$ - chains in solution
$S(q,t) \sim \exp[-(\Gamma t)^{1/2}]$

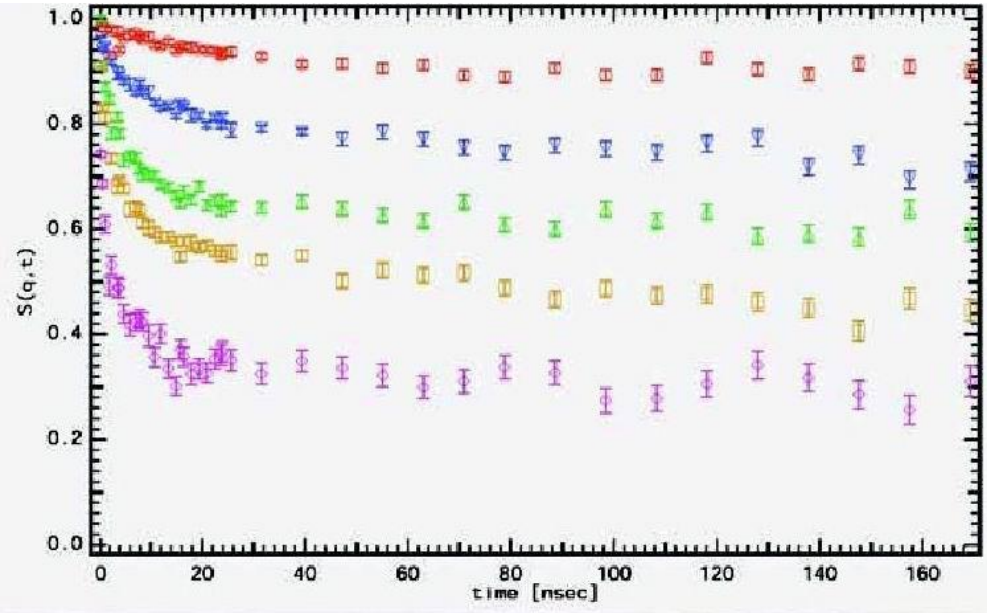

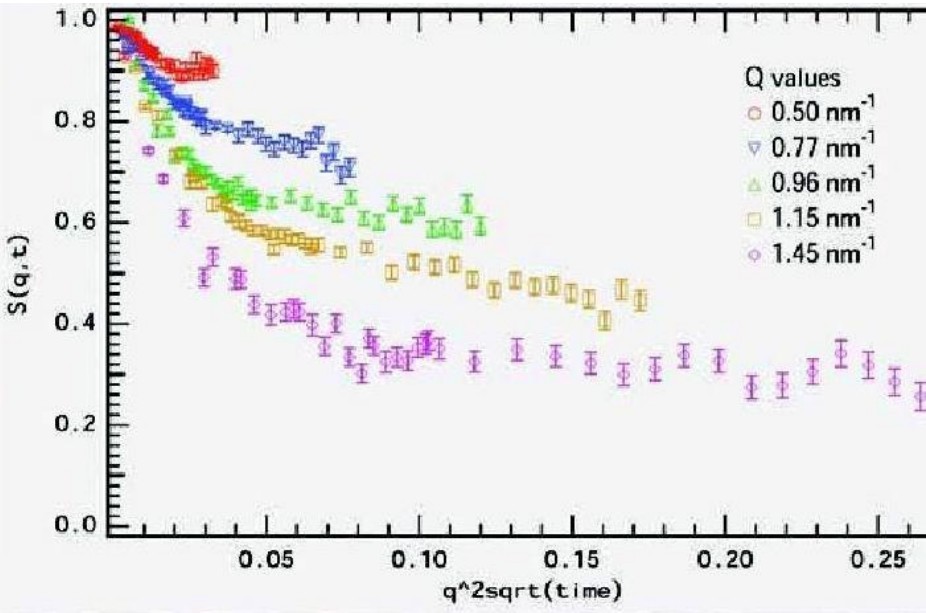

P.Schleger, B.Farago, C.Lartique et al. Phys. Rev. Lett. 81, 124 (1998).
B. Ewen, D.Richter. Neutron Spin Echo Investigation on the Segmental Dynamics of Polymers in Melts, Networks and Solution. Advances in Polymer Science, V. 134. P. 3-129.

Dynamics of gels

Slide-Ring Gel

Okumura and Ito, Adv. Mater. 13, 485 (2001).
Ito, Polymer J. 39, 489 (2007).

polymer (PEG) — cyclodextrine (CD) — bulky end cap

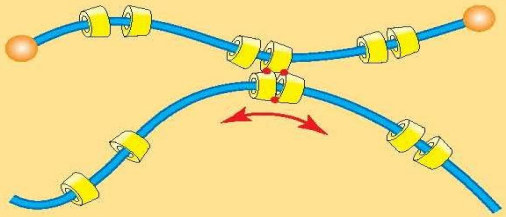

After the introduction of the cross-linking points, the CD can move along the polymer chain: Slide-Ring (SR) Gel

chemical gel

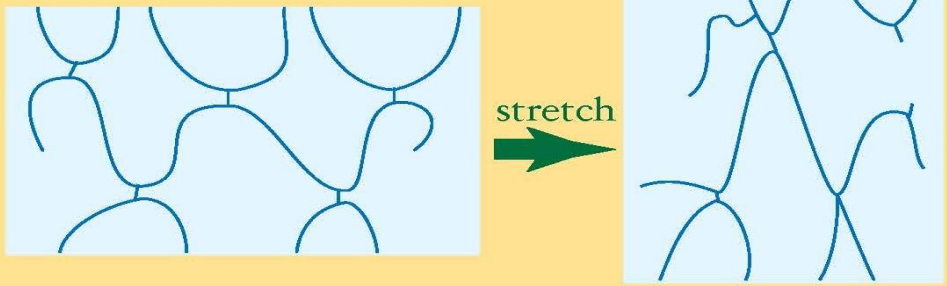

chemical gel: stretching the gel results the break of the polymer chains from the weakest point.

slide-ring gel

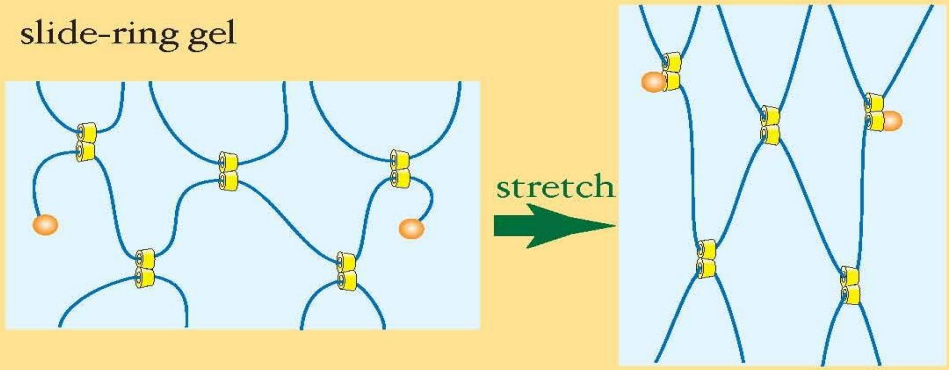

slide-ring gel: stretching the gel results the move of the cross-linking points and internal stress is spontaneously releaved.

high extensibility

large degree of swelling

large reversible deformability

In order to achieve these physical properties, the cross-linking points must slide along the polymer chain with the similar time scale of the polymer dynamics. ----> Sliding motion

Possible dynamics in the Slide-Ring Gel

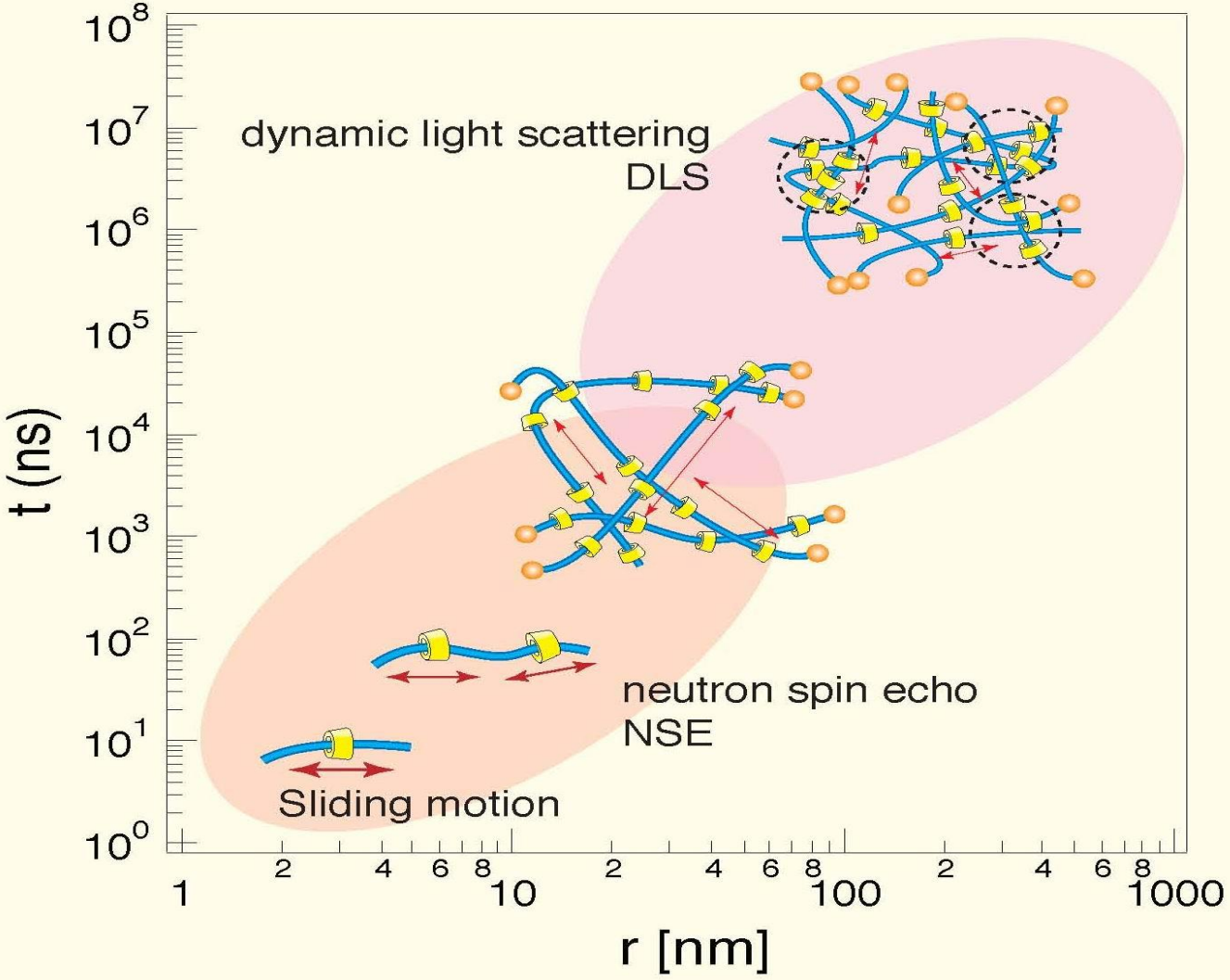

dynamic light scattering (DLS)

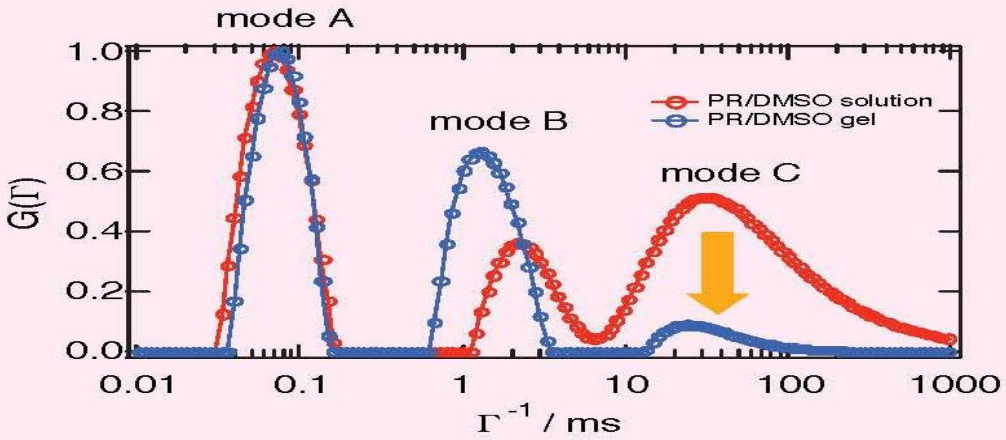

mode A & B: existing both in solution and gel
mode C : disappeared in the gel

mode assignment
mode A: due to the collective dynamics of the PEG chain
mode B: sliding along the PEG chain?
mode C: self-diffusion of CD cluster along the PEG chain

to define local dynamics of the CD molecule
NSE measurement is necessary

Polyrotaxane in NaOD aqueous solution and gel

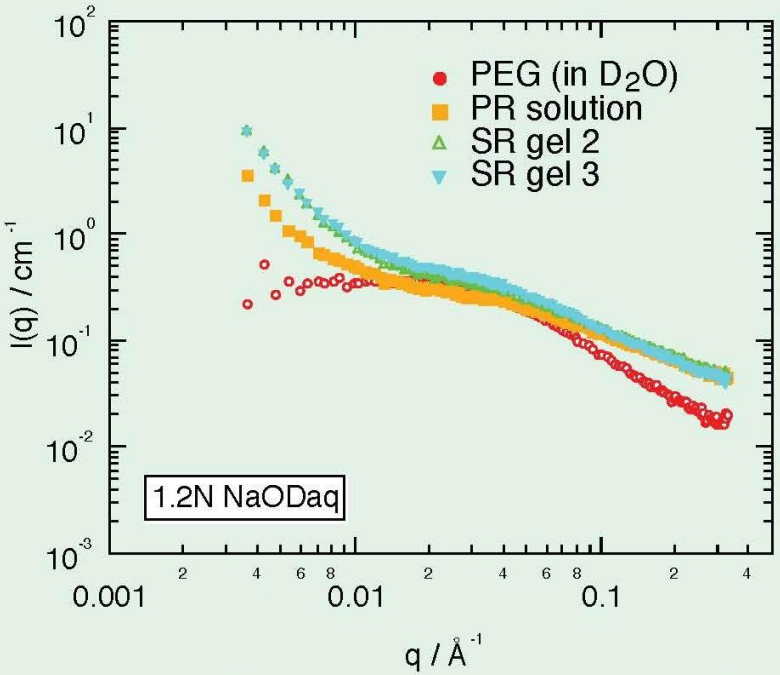

Comparison of the SANS profiles obtained from the PEG in D2O, polyrotaxane in NaOD aqueous solution, and slide-ring gel with the solvent of NaOD and water.

Upturn at low-q for PR solution and SR gel is due to the inhomogeniety of the system. The higher intensity at high-q for PR solution and SR gel is ascribed to be the existence of CD molecules.

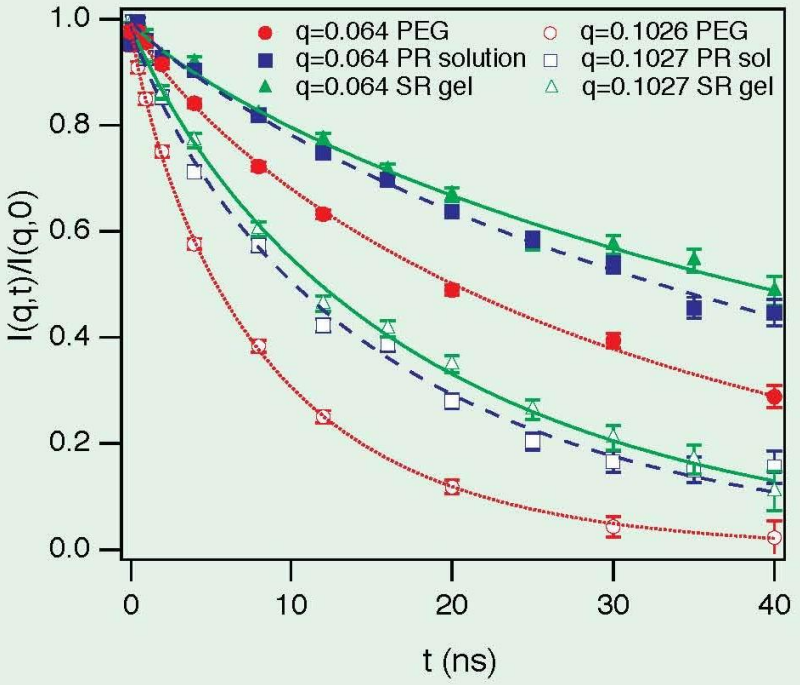

Comparison of the I(q,t)/I(q,o) obtained from the PEG in D2O, polyrotaxane in NaOD aqueous solution, and slide-ring gel with the solvent of NaOD and water.

SR gel < PR solution < PEG in D2O

faster dynamics

q-dependence of the initial decay rate Γ of the $I(q,t)/I(q,0)$

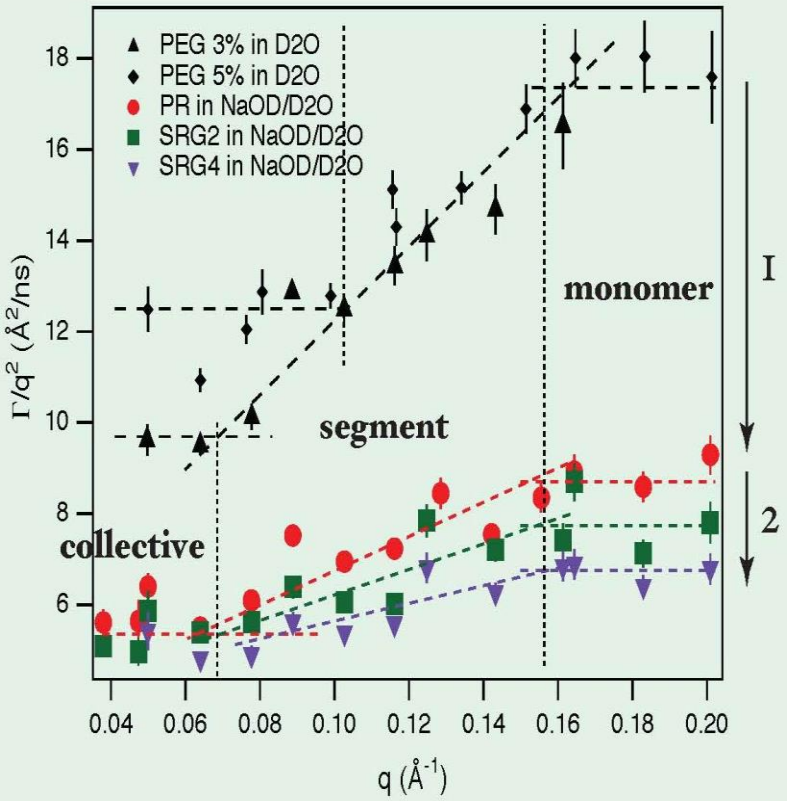

collective mode -> segment mode -> monomer diffusion

suppression of dynamic mode

1. Strong suppression due to the association with CD
2. Slight suppression due to the introduction of cross-linking points

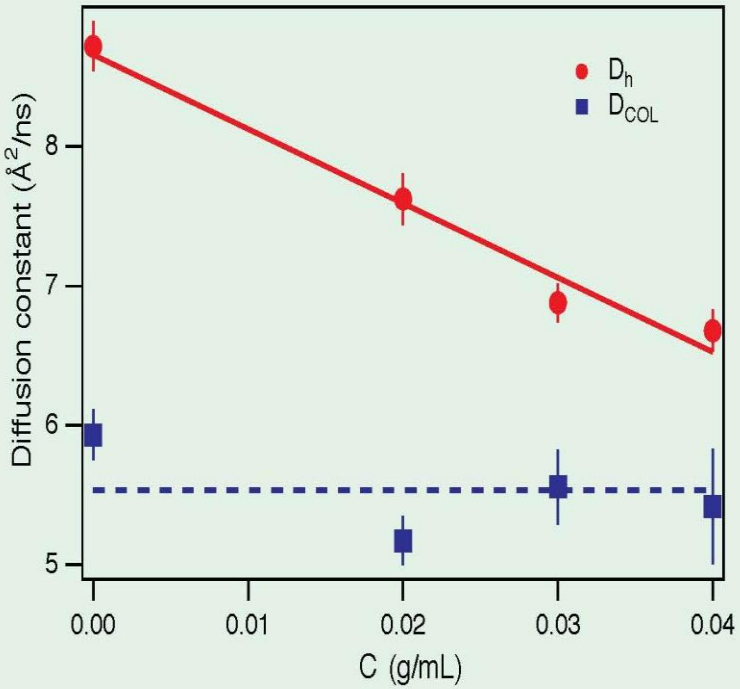

Diffusion constant at low-q: collective mode, D_{COL} almost constant with cross-linker concentration, C.

Diffusion constant at high-q: sliding mode?, D_h linear decrease with cross-linker concentration, C.

Necessary to decouple contributions between polymer chain and CD molecules since the time scale of the motion of polymer and CD is close to each other

contrast variation technique in the SR gel systems

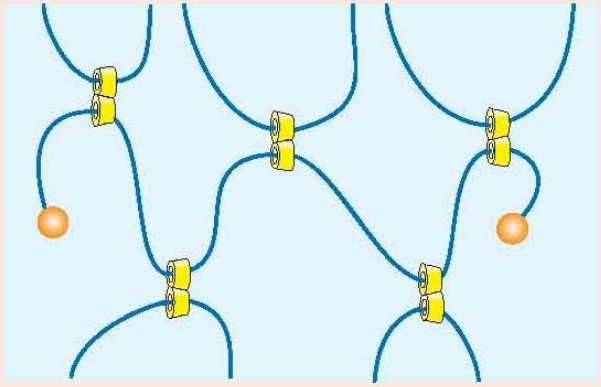

original contrast
h-PEG/h-CD/d-DMSO
abbrebiated by h-PR

polymer-polymer correlation is dominated in the scattering profile

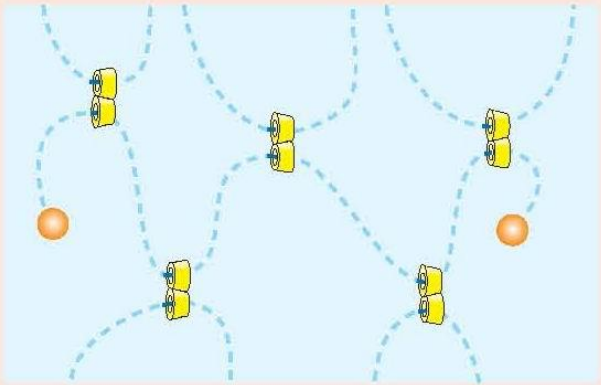

CD contrast
d-PEG/h-CD/d-DMSO
abbrebiated by d-PR

CD-CD correlation is more visible in the scattering profile

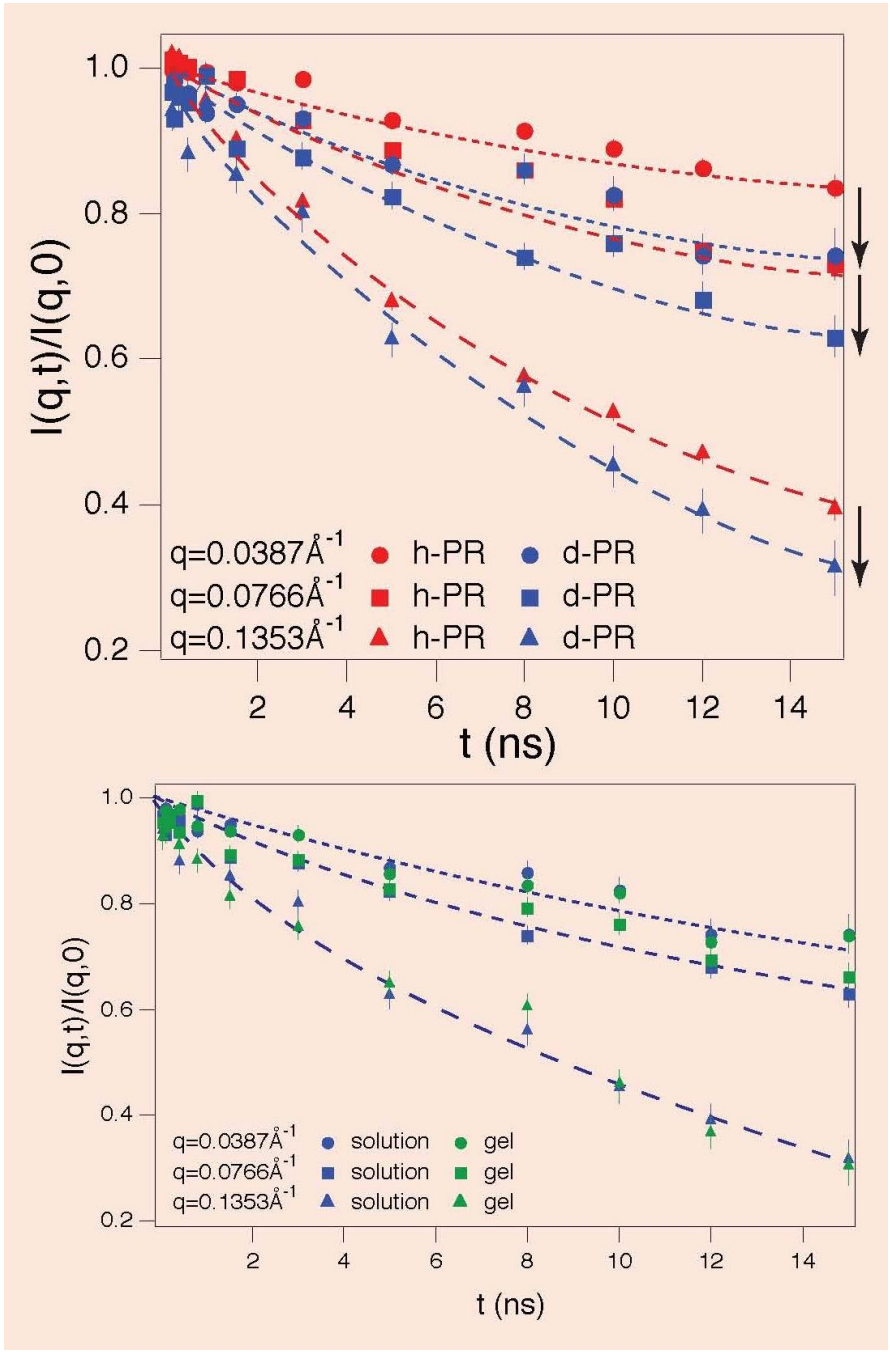
1.0
0.8
0.6
0.4
0.2
I(q,t)/I(q,0)
q=0.0387Å-1 h-PR d-PR
q=0.0766Å-1 h-PR d-PR
q=0.1353Å-1 h-PR d-PR
2
4
6
8
10
12
14
t (ns)
1.0
0.8
0.6
0.4
0.2
I(q,t)/I(q,0)
q=0.0387Å-1 solution gel
q=0.0766Å-1 solution gel
q=0.1353Å-1 solution gel
2
4
6
8
10
12
14
t (ns)

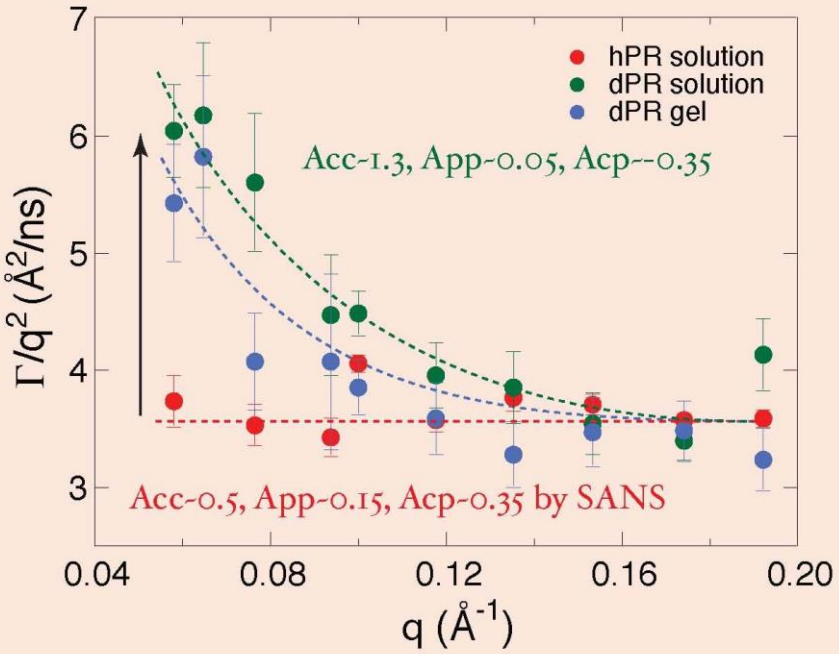

$$\Gamma(q) = A_{cc}(q)\Gamma_{cc}(q) + A_{pp}(q)\Gamma_{pp}(q) + A_{cp}(q)\Gamma_{cp}(q)$$

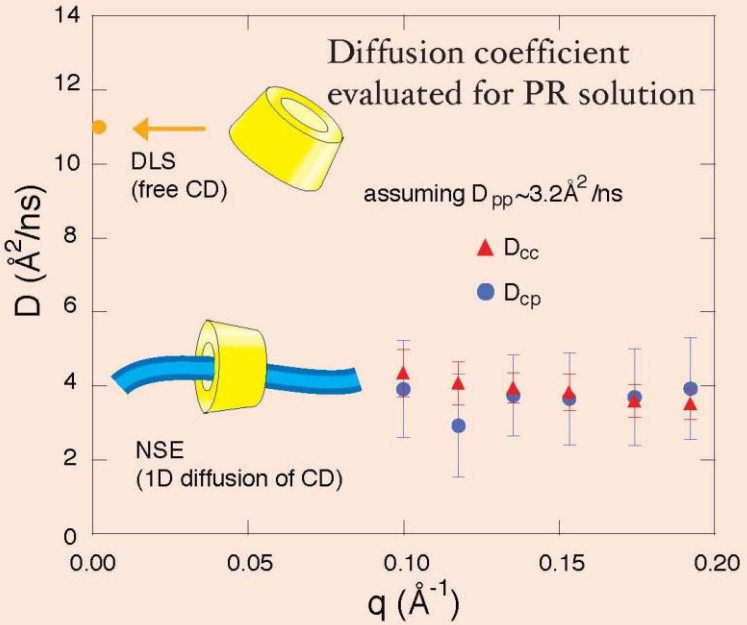

Neutron Spin Echo study of Deformations of Spherical Droplets*

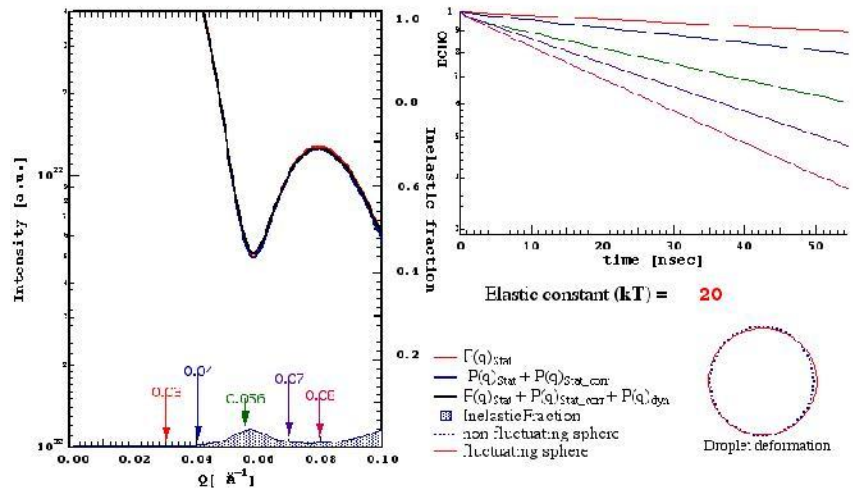

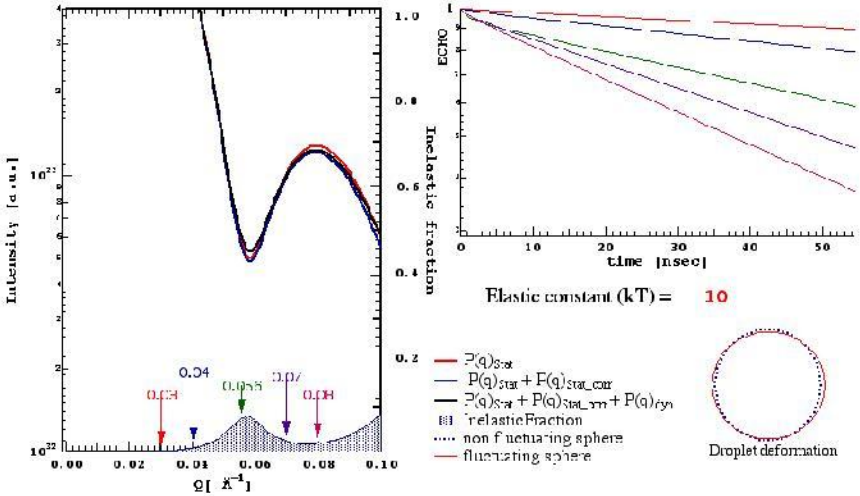

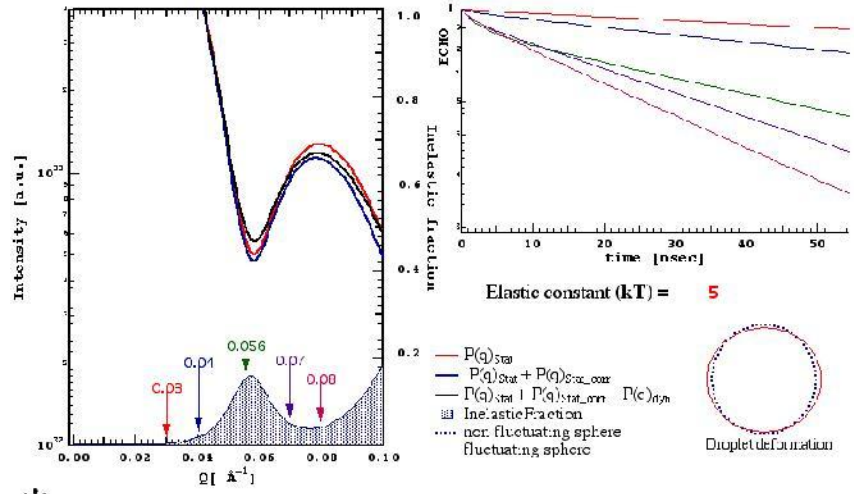

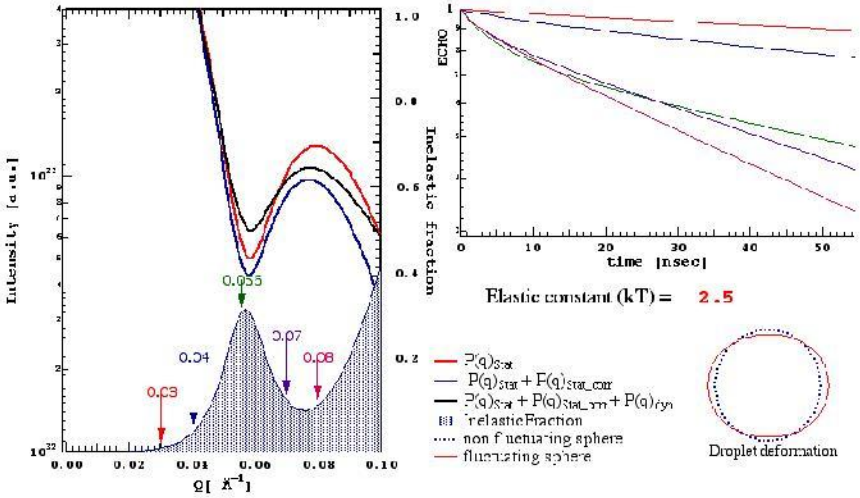

* Courtesy of B. Farago

Феррожидкости с низкой T_C

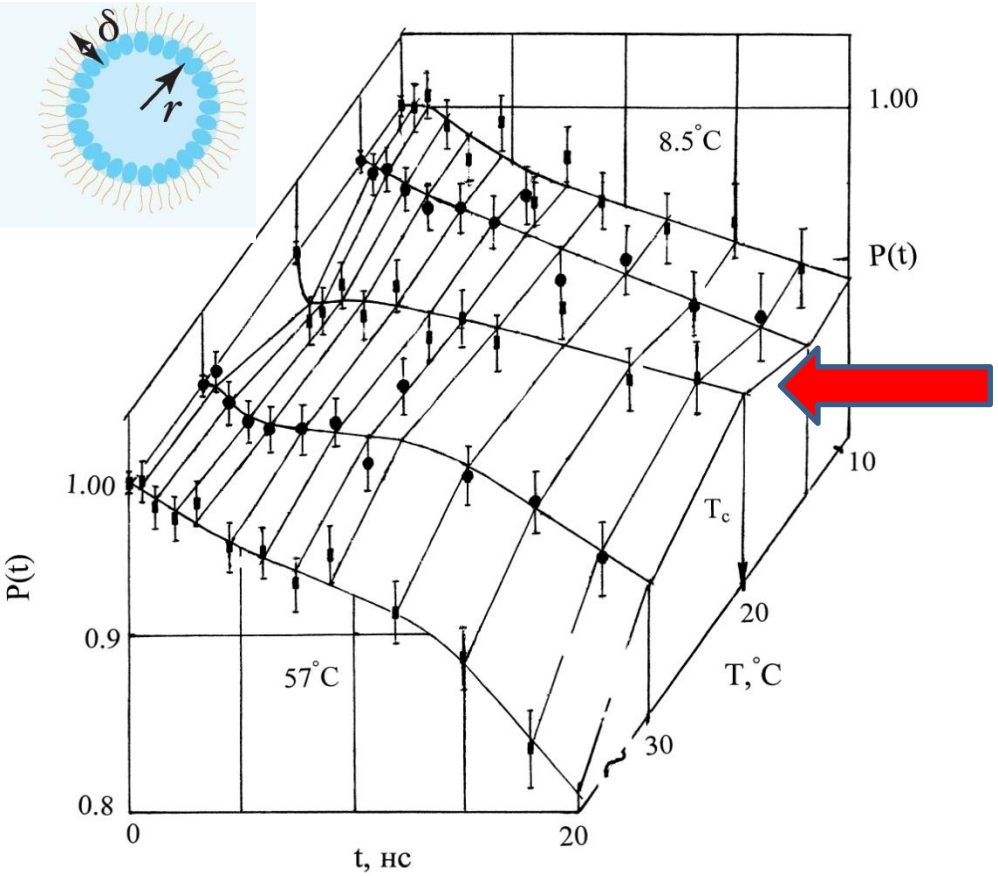

NSE-сигнал от ФЖ1 в зависимости от времени и температуры, q = 1 нм$^{-1}$. Линии - сплайн-функции

$P(t,q) = \exp[-q^2 \cdot R^2(t)/2]$,

$R^2(t)=r_o^2+2D_F \cdot t$ - квадрат смещения частицы

r_o - амплитуда быстрых колебаний,

D_F - константа диффузии частицы

Переход через точку Кюри магнитной фазы (**$T > T_C$**): магнитные силы исчезают, действуют силы ван-дер-Ваальса, электростатические, стерического отталкивания

Эффект критического замедления диффузии !

V.T. LEBEDEV, GY. TÖRÖK .Effect of *anomalous particles diffusion damping* in *ferrofluid near Curie temperature. // Romanian Report in Physics. V. 58, N 3 (2006)*

Ферриты с низкой **T_C**:

$Me_XZn_{1-X}Fe_2O_4$ (Me ≡ Mn,Ni,Co)

ФЖ1 :Частицы $Mn_{0.3}Zn_{0.7}Fe_2O_4$ (R_P = 10 нм, $\Delta R_P/R_P$ = 0.5) в додекане: **T_C = 20 °C**, ПАВ - олеиновая кислота, объемная доля частиц C = 8 %, намагниченность феррита $4\pi M$ = 16 Гс (17 °C)

ФЖ2: $Mn_xZn_{1-x}Fe_2O_4$, x ~ 0.3, R_P = 5 нм, **T_C = 16 °C**, ПАВ-олеиновая кислота, носитель - додекан, C = 15 % объемн.

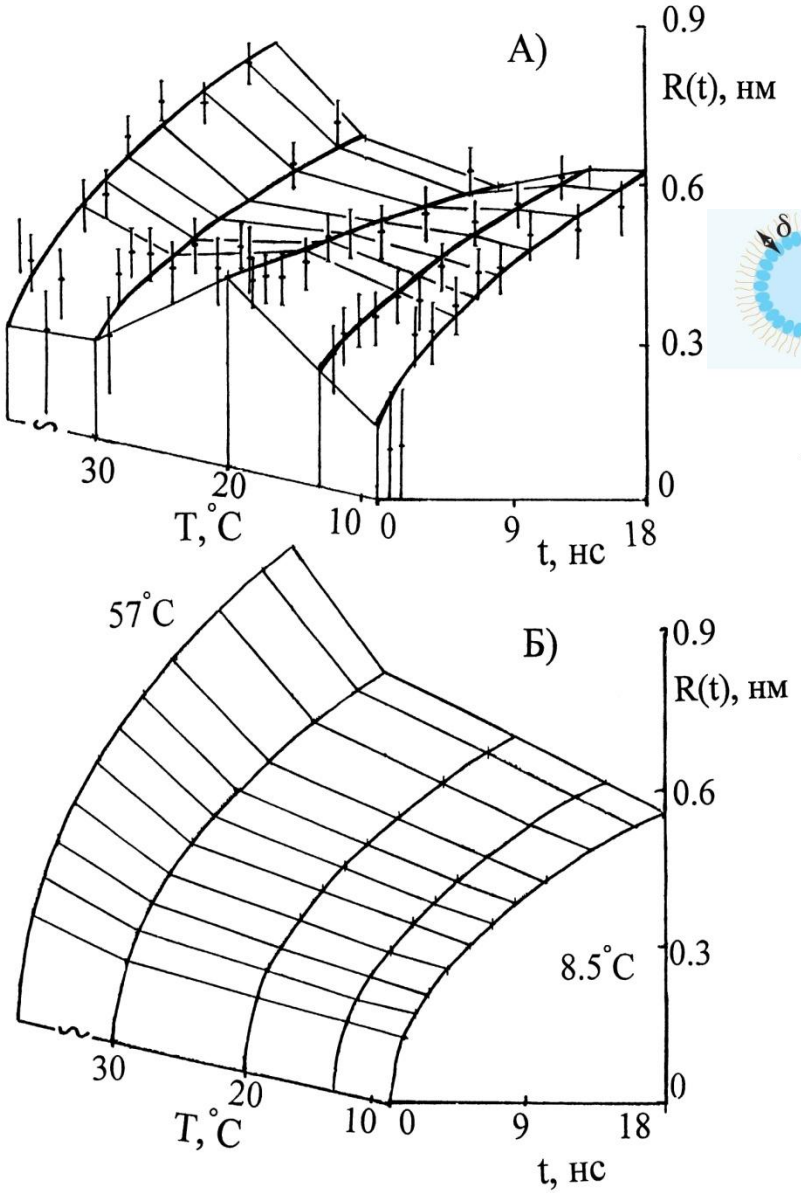

Измеренные (А) и расчетные (Б) смещения частиц - функции времени и температуры

ФЖ1. T = 8-60 °C: А) $r_0^2(T)$ - квадрат амплитуды колебаний; Б) $D_F(T)$ - константа диффузии; прерывистая линия - свободная диффузия

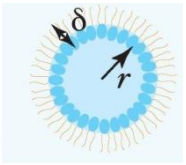

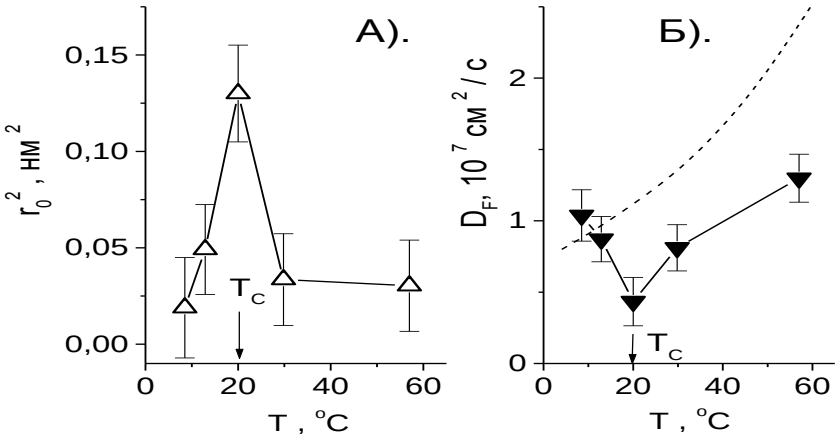

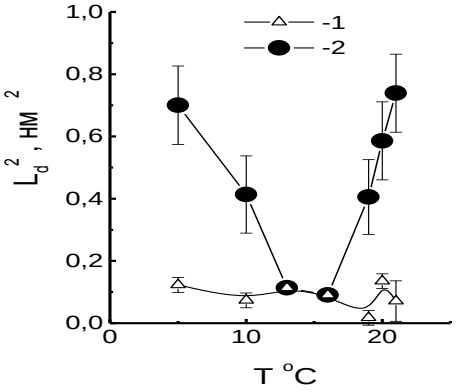

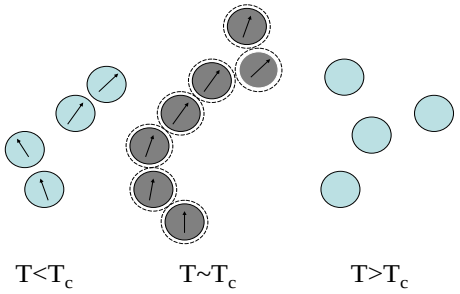

ФЖ2: квадрат диффузионной длины в зависимости от температуры при быстрой (1) и медленной (2) динамике

NSE in biology

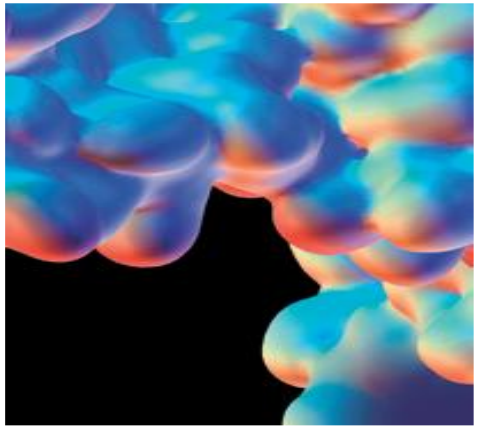

Enzyme Research

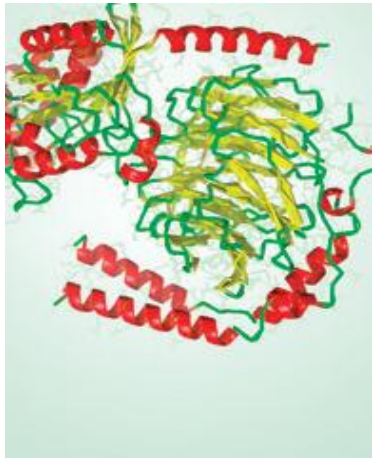

Signal Transduction

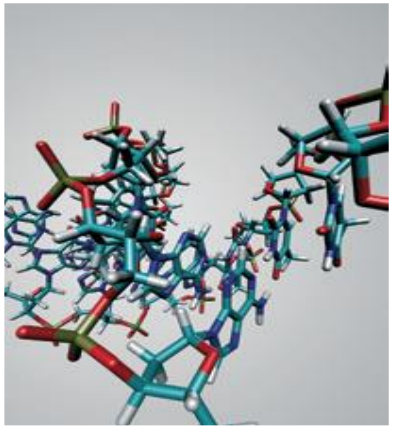

Nucleic Acids

Biochemistry

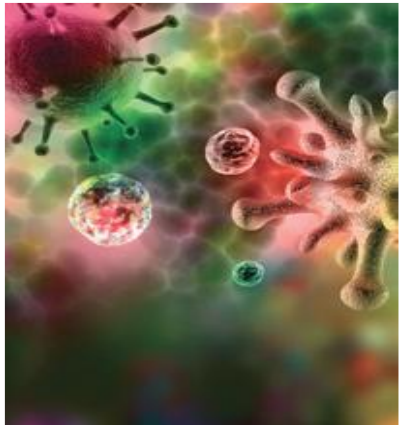

Virology

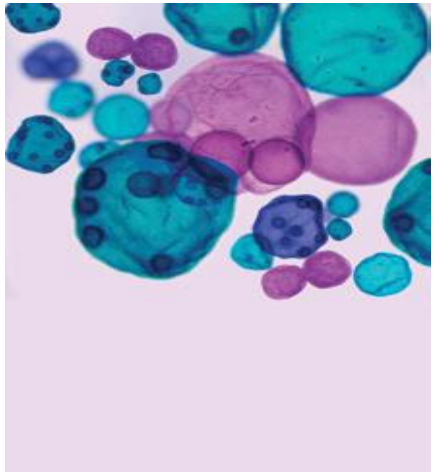

Microbiology

Genetics

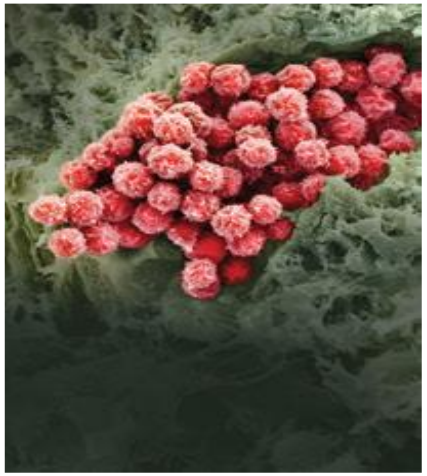

Stem Cells

Mesoscopic Membrane Fluctuations

Dispersion relation

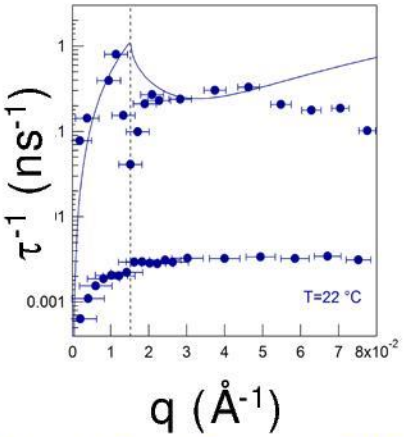

Contains 'dynamic' information

q-dependence of excitation frequencies and relaxation rates

Thermal membrane fluctuations

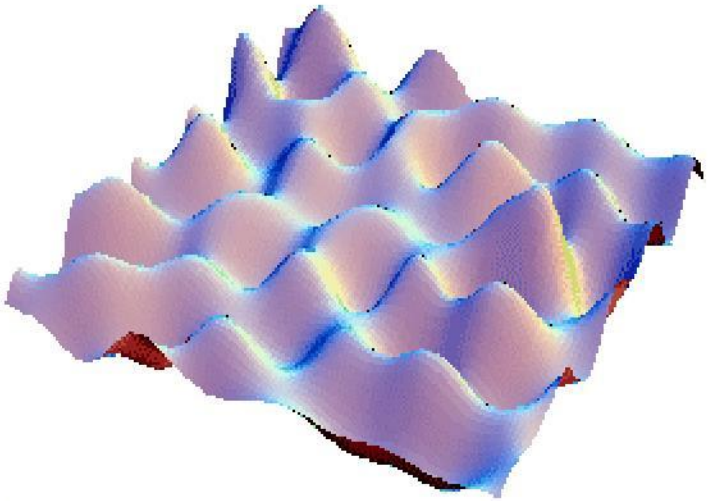

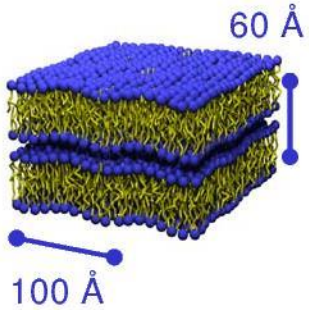

Elementary excitations

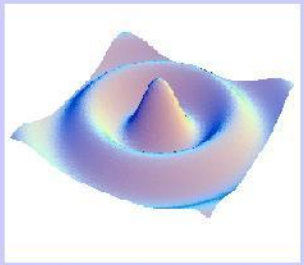

Propagating

+

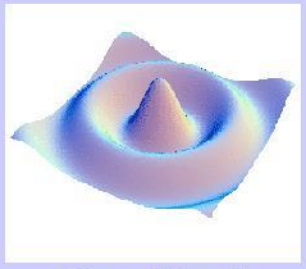

Oscillating

+

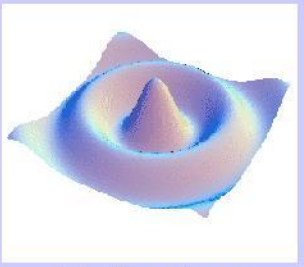

Relaxing

Mode

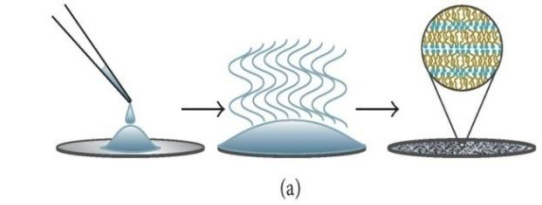

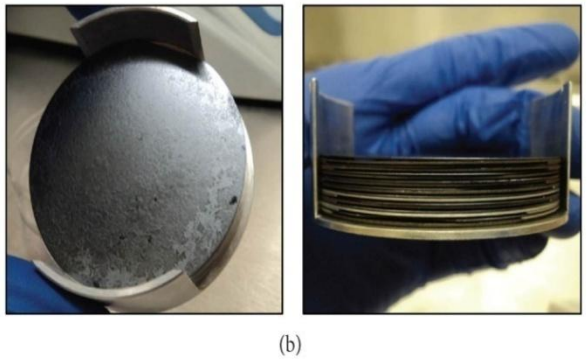

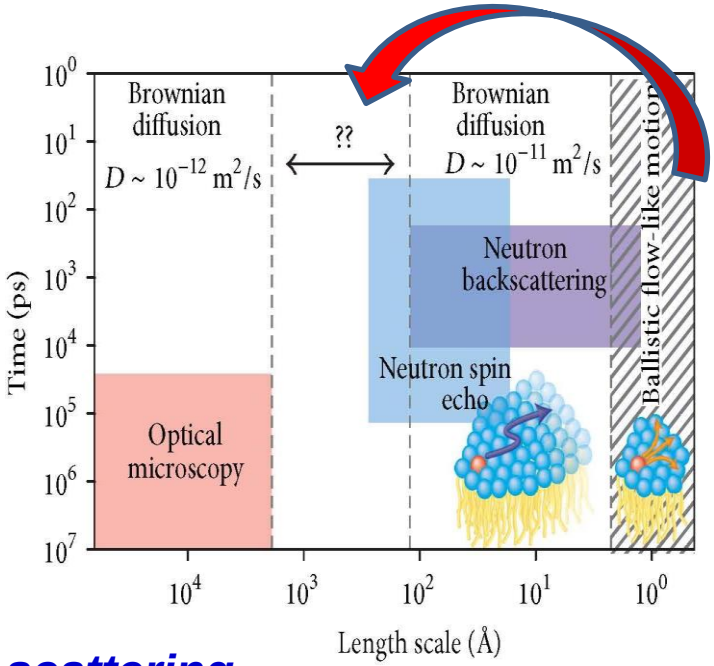

Lipid motion:

A gap from ≈ 10nm to ≈ 200 nm

between the fluorescence measurements and neutron backscattering

Difference in the diffusion coefficients observed on each side of this gap

Coherent and Incoherent scattering

- Correlations between atoms (interactions)
- Correlations between the positions of the **same nuclei at different times** - **dynamics of a particle**

NSE:

high energy resolution + low scattering vectors to study long-range diffusion

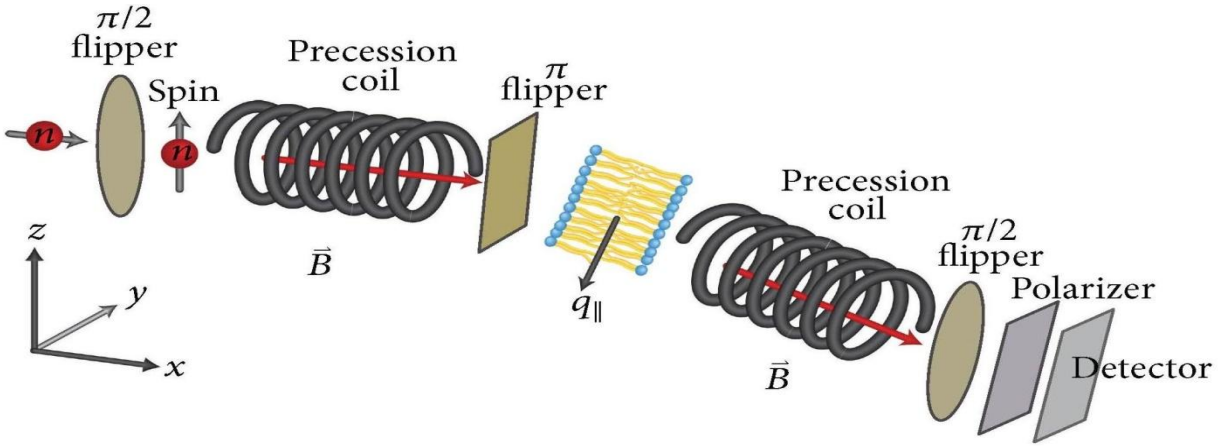

C. L. Armstrong, L. Toppozini, H. Dies, A. Faraone, M. Nagao, M. C. Rheinstädter.
Incoherent Neutron Spin-Echo Spectroscopy as an Option to Study Long-Range Lipid Diffusion.// Hindawi Publishing Corporation ISRN Biophysics, Volume 2013, Article ID 439758, 9 pages, http://dx.doi.org/10.1155/2013/439758

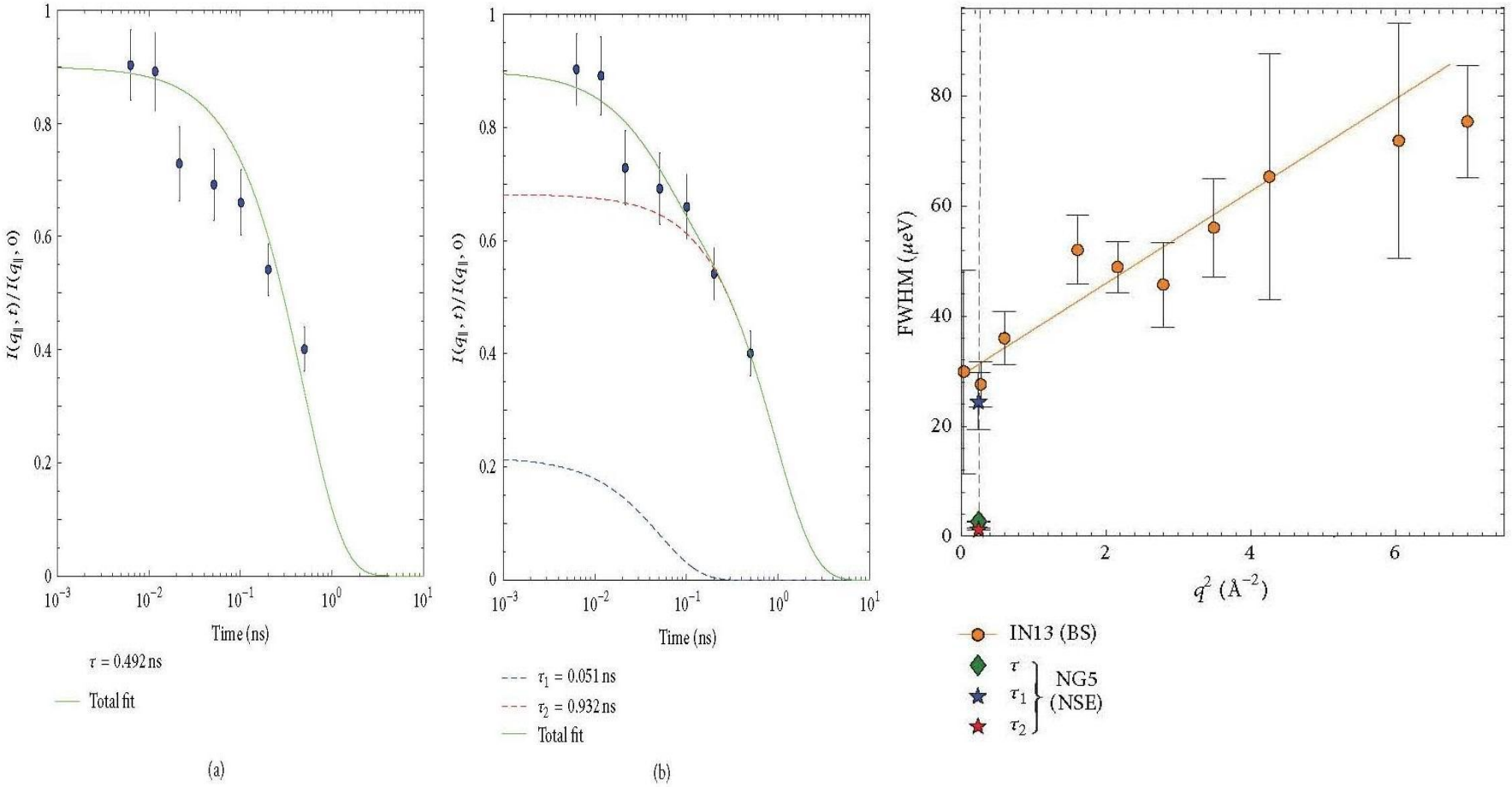

***Lipid diffusion*: incoherent neutron scattering and fluorescence microscopy**

- **Lipids move coherently** in loosely bound clusters, rather than as independent molecules
- **"Hopping" diffusion of lipids into nearest neighbour** sites was observed in single supported bilayers
- **Flow-like component** to the motion of the lipid molecules over long length scales

Lateral Self-diffusion of lipids

1,2-dimyristoyl-sn-glycero-3-phosphocholine (DMPC) *in plane of membrane*

Highly **oriented membranes** prepared on **silicon wafers** and **aligned**
Incoherent NSE: protonated membranes hydrated with **D_2O**

A solution of 20 mg/mL DMPC in 1 : 1 chloroform and 2,2,2-trifluoroethanol (TFE) prepared, pipetted onto each Si wafer and allowed to dry

The wafers were kept in vacuum overnight to remove all traces of the solvent
The samples were then hydrated with D_2O, and annealed in an incubator at 308K for 24 hours

3000 highly oriented stacked membranes with a total thickness of ≈10 micrometer
Eight Si wafers were stacked with 0.6 mm aluminium spacers placed in between each wafer to allow the membranes to be hydrated, creating a 10% scatterer

$$S(q_{||},t)/S(q_{||},0) = A_1 exp(-t/\tau_1) + A_2 exp(-t/\tau_2)$$

Faster diffusion, τ_1 **= 0.05 ns**, of an **individual lipid**, confined within a domain
Slower process of a lipid τ_2 **= 0.9 ns** moving as **part of domain**

Dynamics of model membranes

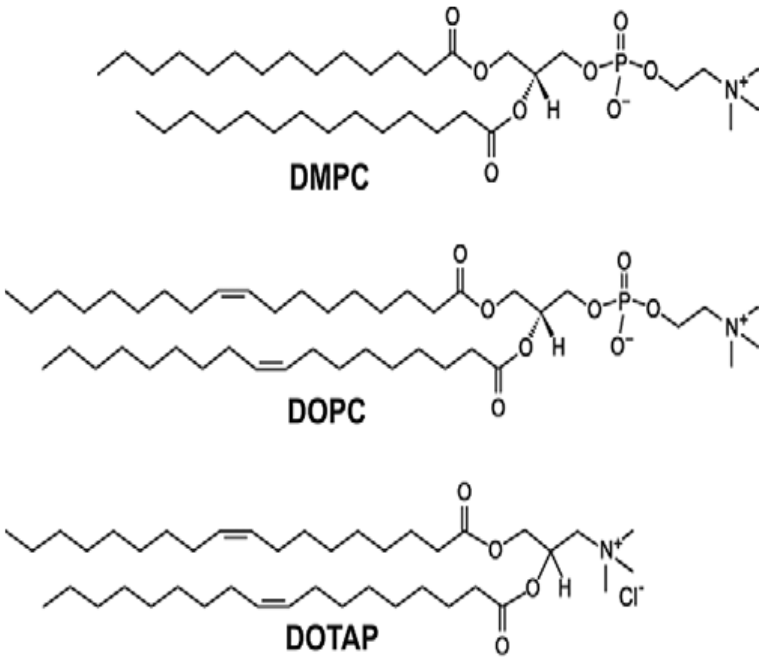

B. Bruning, R. Stehle, P. Falus, B. Farago.
Influence of charge density on bilayer bending rigidity in lipid vesicles: A combined dynamic light scattering and neutron spin-echo study.
// Eur. Phys. J. E (2013) **36**: 77

Lipid molecules

DMPC (1,2-dimyristoyl-sn-glycero-3-phosphatidylcholine) – ***saturated, uncharged***

DOPC (unsaturated, uncharged)
DOTAP - cationic lipid 1,2-dioleoyl-3-trimethylammonium-propane
unsaturated

NSE-study: vesicles of lipids

Bilayer's **mechanical properties and undulation** dynamics can be tuned by changing its composition through lipid headgroup or acyl chain properties

Undulation dynamics in lipid vesicles composed of DMPC/DOTAP and vesicles composed of a mixture of the uncharged helper lipid DMPC with the also uncharged reference lipid 1,2-dioleoyl-sn-glycero-3-phosphocholine (DOPC).

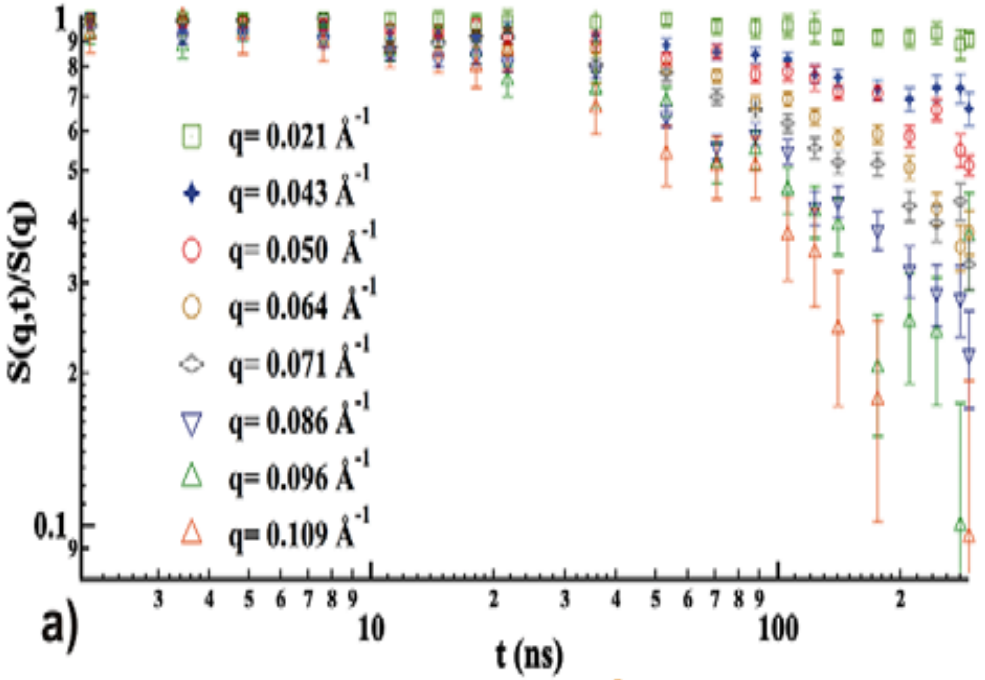

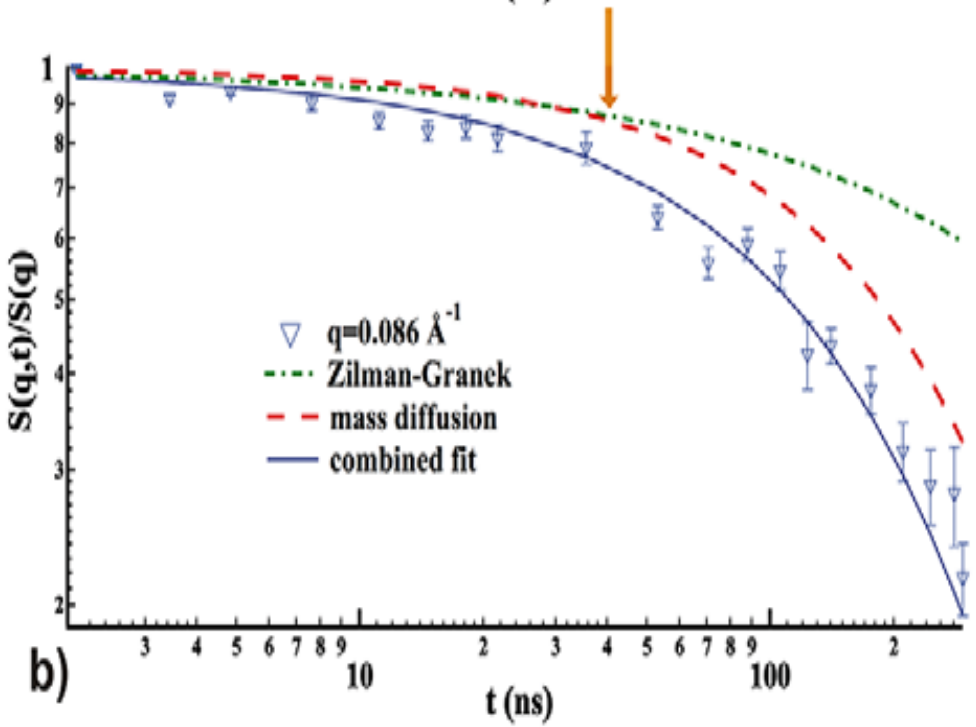

Scattering functions

***S*(*q*, *t*)/*S*(*q*)** for **DMPC** at 30 ◦*C*

(a) *q*-range at λ = 1.8 nm
(b) combined fit:
vesicle center-of-mass diffusion
+ bilayer undulations

Dynamic light Scattering
hydrodynamic vesicle radii
***R_H* ~ 45-55 nm**
At intermediate concentrations of the cationic lipid DOTAP (20 - 40 mol%), vesicles quickly increased size to radii up to **70 and 80 nm**

Stokes-Einstein equation

$$R_H = k_B T / 6\pi \cdot \eta(T) \cdot D$$

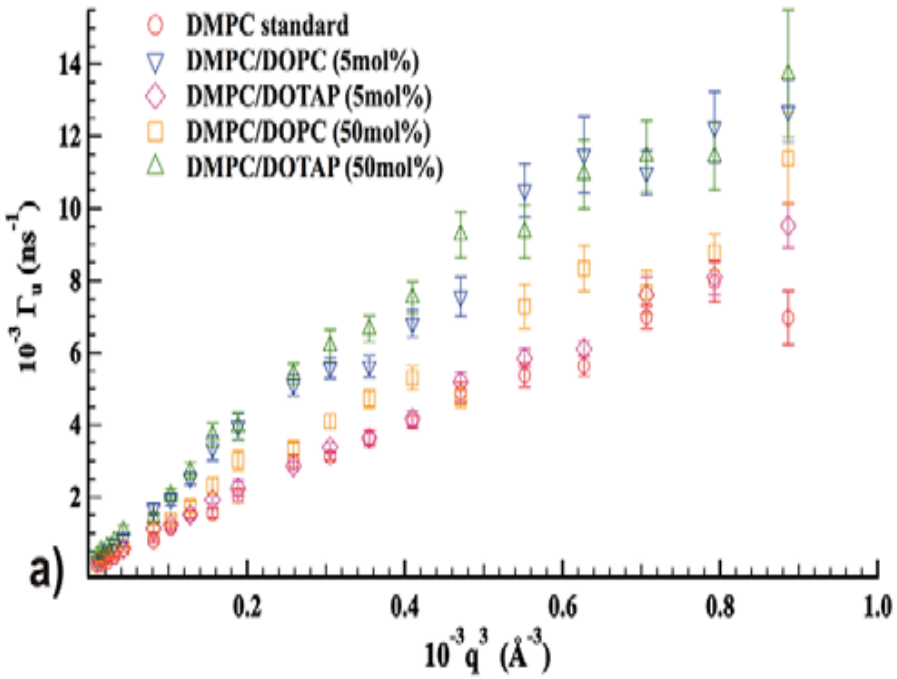

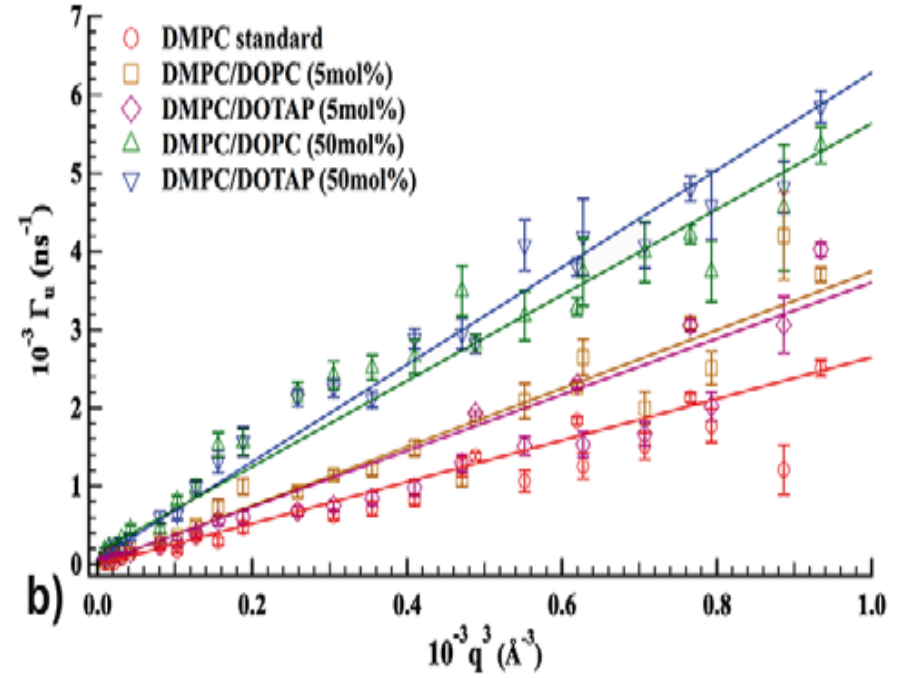

Fluctuation dynamics: droplets, vesicles S.T. **Milner**, S.A. **Safran**, Phys. Rev. A **36**, 4371 (1987), ***MS-approach***

Normal bending modes of the **flexible interface** are coupled to the viscous friction:

$$\exp(-\Gamma_{MS}t),\ \Gamma_{MS} = (\kappa/4\eta)q^3$$

η - effective viscosity of solvent

κ - bilayer bending rigidity

Rigid membrane $\kappa >> k_BT$

Stretched decay

$$S(q, t) \sim \exp[-(\Gamma_u(q)\cdot t)^{\beta}]$$

$$\Gamma_u = 0.025\gamma_q\,(k_BT/\kappa)^{1/2}\,[kBT/\eta(T)]q^3,\ \gamma_q \sim 1$$

$$S(q, t)/S(q, 0) = A\cdot\exp(-\Gamma_d t)\cdot\exp[-(\Gamma_u t)^{\beta}]$$

$\Gamma_d = D\cdot q^2$ *center-of-mass diffusion rate*

Γ_u - *relaxation rate of bilayer undulations*

stretched exponential, $\beta = 0.66$

Zilman-Granek approach

• ***Softening*** : Small amounts of added ***unsaturated lipid*** (5 % DOPC, DOTAR) evoke a ***distinct decrease*** (3 times) in the bilayer bending ***rigidity***

$$\kappa \sim \Gamma_u / q^3$$

Lipid headgroup charge does not cause the most prominent changes in the bilayer bending rigidity

Bilayer softening - heterogeneity of the mixture: mismatch between the hydrophobic acyl chains of the respective lipids, which causes a lateral segregation in the membrane plane (domain formation)

Domain structure fluctuations and bilayer bending rigidity

Increasing amount of inserted unsaturated lipid → ***Fluidization of the membrane***

Biomedical aspects

Cationic liposomes, which are more suitable as carrier vehicles than their zwitterionic counterparts, do not suffer from increased instabilities through their headgroup charges

M. Mell, L. H. Moleiro, Y. Hertle, P. Fouquet, R. Schweins, I. Lopez-Montero, T. Hellweg, F. Monroy. ***Bending stiffness of biological membranes: What can be measured by neutron spin echo?*** Eur. Phys. J. E (2013) **36**: 75

Vesicles (extrusion) - adequate membrane models

NSE: *Shape fluctuations around the spherical average topology*

Height-to-Height autocorrelation function

$$< h_q(t)h_{-q}(0)> = <h^2_q>B\ exp[-\omega_B(k)t]$$

Bending mode amplitude

thermal energy / elastic energy $<h^2_q>_B = (k_BT)/(\kappa q^4)$

q^3-dependent relaxation rate → **bending stiffness**

$$\omega_B(q) = (\kappa/4\eta)q^3 \sim \kappa$$

Bending modes appears as a series of internal modes - **shape fluctuations**

Spherical membranes - vesicles, emulsion droplets

Intermediate scattering function

$$S(q, t) = \exp[-\Gamma_T t]\,[A_T(q) + A_B(q) S_B(q, t)]$$

$\Gamma_T = D_T q^2$ - diffusive rate of the translational motion

Normalization : $A_T + A_B = 1$

Dynamics dominated by bending modes: $\langle h_q^2 \rangle \sim q^{-4}$, $\omega_q \sim q^3$

1. Rigid membranes: $\kappa >> k_B T$

Bending modes are extremely weak

Stretched relaxation might arise from the **sum of modes**

2. Floppy membranes: $\kappa \longrightarrow 0$

Large shape fluctuations

Single spherical mode dominates $S(q, t) \approx \exp(-\Gamma_{MS} t)$

$\Gamma_{MS} \approx \omega_B = (\kappa/4\eta) q^3$

Tipical Lipid bilayers: $\kappa \sim (5\text{–}20) k_B T$

Gaussian distribution of the averaged fluctuations
Dynamic structure factor

$$\langle \exp(iq\Delta h(t)) \rangle = \exp[-q^2\langle \Delta h^2(t)\rangle/2],\ \langle \Delta h^2(t)\rangle \approx (Dt)^{2/3}$$

Rigid membranes: shape fluctuations **-** ***sub-diffusive dynamics***
slower than a free diffusion in soft membrane

A.G. Zilman, R. Granek, Phys. Rev. Lett. **77**, 4788 (1996)
R. Granek, J. Phys. II **7**, 1761 (1997)

Effective diffusion coefficient $D \approx 0.025(k_BT/\kappa)^{1/2}(k_BT/\eta)q$

Intermediate scattering function

$$S(q,t) \approx \exp[-(\Gamma_{ZG}t)^{2/3}] \qquad \Gamma_{ZG} \approx 0.025(k_BT/\kappa)^{1/2}(k_BT/\eta)q^3$$

Summed correlations over different modes, $\Gamma_{ZG} \sim \kappa^{-1/2}$,

differently from the relaxation rates of the **individual modes** $\omega_B \sim \kappa$

$$S(t) = \exp(-D_T q^2 t)\{ A + (1 - A)\exp[-(\Gamma_{ZG}t)^{2/3}]\}$$

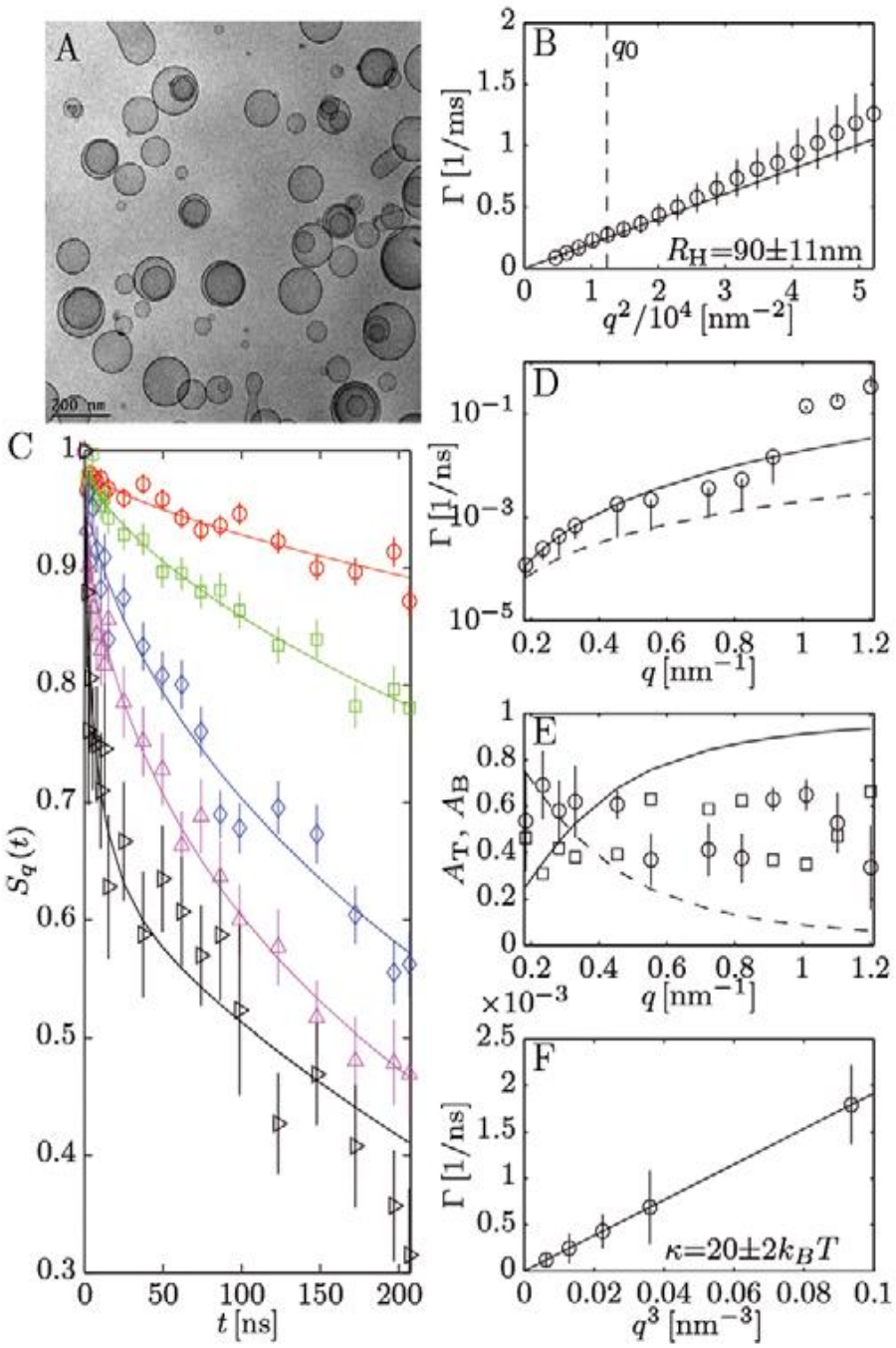

Vesicles made of phosphocholines

with increasing melting temperature

SMPC (*Tm* = 30°C) (rigid)

DMPC (*Tm* = 23°C) ***Tm***

POPC (*Tm* = −2°C) (soft)

Higher ***Tm*** indicates increasing molecular cohesion

Bilayers must become **stiffer !!!**

Not rigid membranes

A) CryoTEM image of ***DMPC vesicles*** (extrusion)

B) Relaxation frequencies from DLS, $\Gamma_T = D_T q^2$

C) NSE data, **q = 0.282;0.454;0.723;0.913;1.011 nm**

D) relaxation frequencies of the shape fluctuations

E) amplitudes of translation, *A*, and internal mode corresponding to shape fluctuations, 1 − *A*. Dashed line - relaxation frequency of the translational mode extrapolated to the NSE domain, $\Gamma_T = D_T q^2$ from DLS

F) $\Gamma \sim q^3$, $\kappa = (20 \pm 2) k_B T$

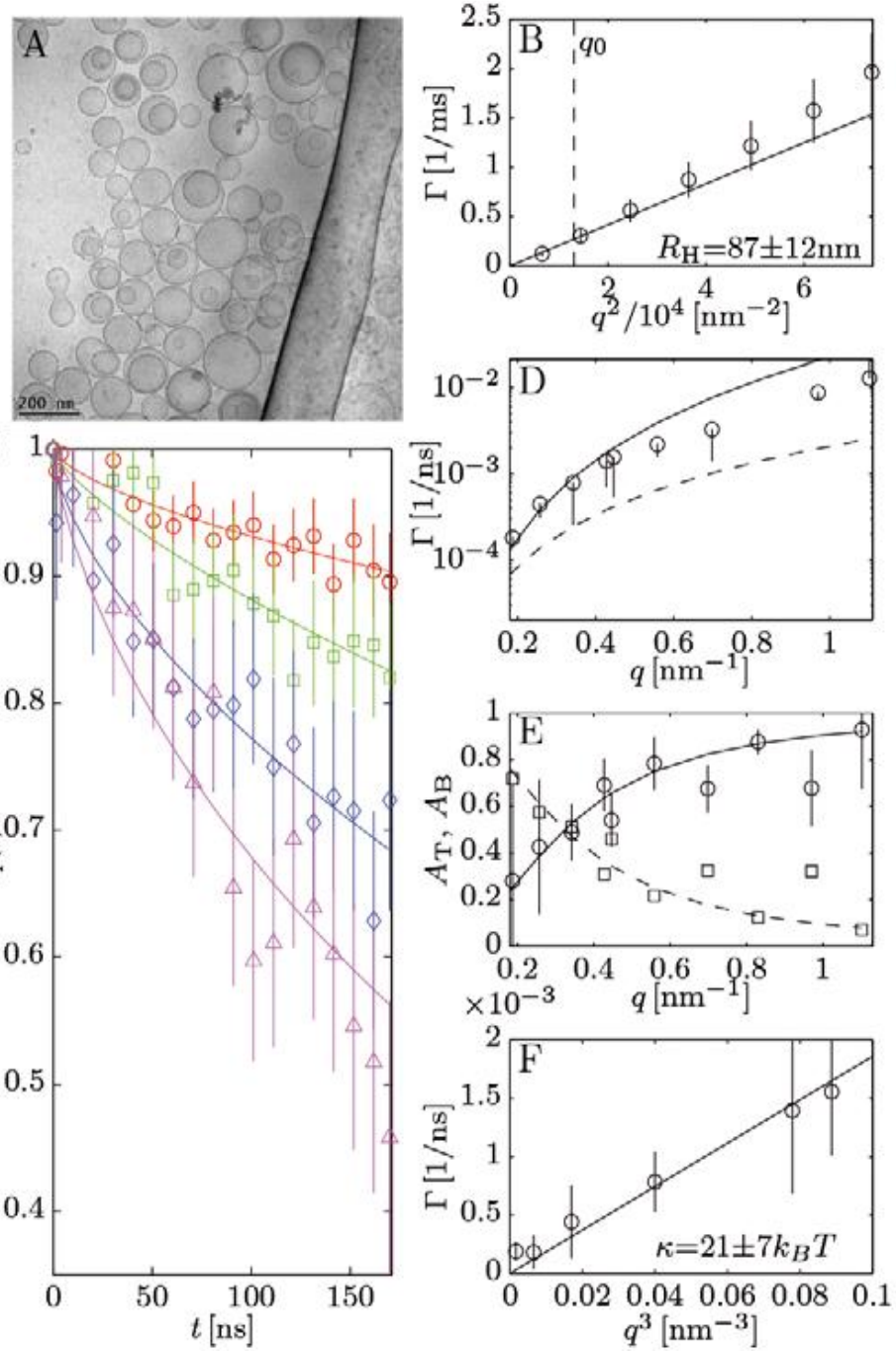

Soft membranes

A) CryoTEM image of ***POPC*** vesicles (extrusion)
B) Relaxation frequencies from DLS

C) NSE data with the fits, which yield the relaxation frequencies D) (***q* = 0.119; 0.558; 0.830; 0.970** nm), E) amplitudes of translation and bending,
F) $\Gamma \sim q^3$

POPC bilayers are expected to be slightly softer under compression and more fluid ($K_{POPC} \approx$ 100mN/m [63]; ***Tm* = −2 ◦C**) than those of DMPC ($K_{DMPC} \approx$ 140mN/m [64]; ***Tm* = 23 ◦C**).
Sliding between bilayers !

Hybrid dynamics in *POPC* bilayers

Bending stiffness $\kappa = (21 \pm 7) k_B T$

Rigid solid-like bilayers

SMPC below its melting point T_m = 30°C
Gel bilayers at 25°C

SMPC vesicles behave as **solid shells** able to undergo **weak shape fluctuations** by contrast to **floppy vesicles** with a fluid membrane of **DMPC or POPC**

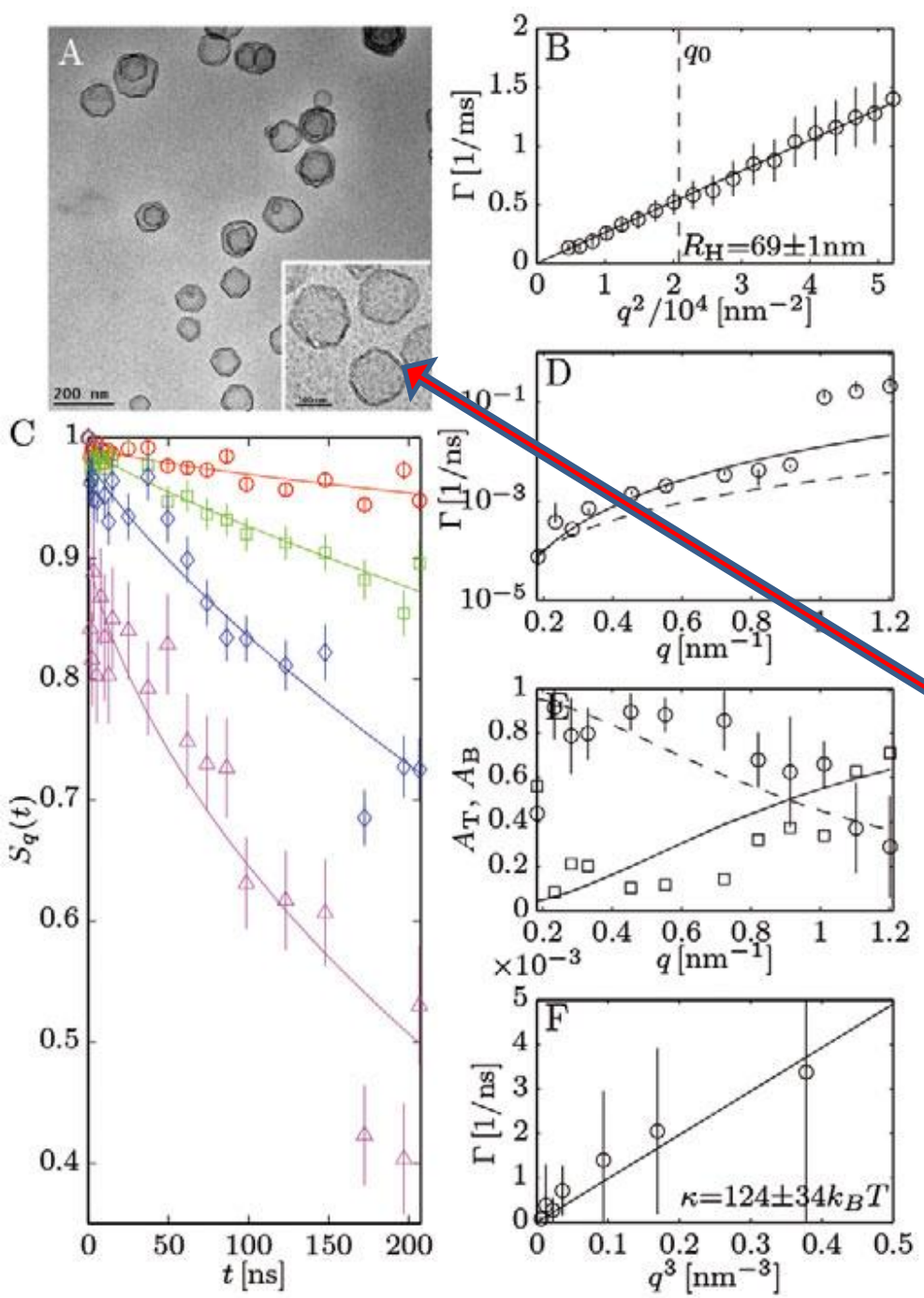

A) CryoTEM image of SMPC vesicles obtained by extrusion
Straight borders along the vesicles contours indicate that they were in the **gel state** at room temperature before being vitrified
B) Relaxation frequencies from DLS data

C) NSE data with the fits, which yield the relaxation frequencies,
***q* = 0.184; 0.454; 0.723; 0.913 nm**
D) Amplitudes of translation and bending;
F). $\Gamma \sim q3$

$$\kappa = (124 \pm 34) k_B T$$

High constant !

Soft Polymer Membranes

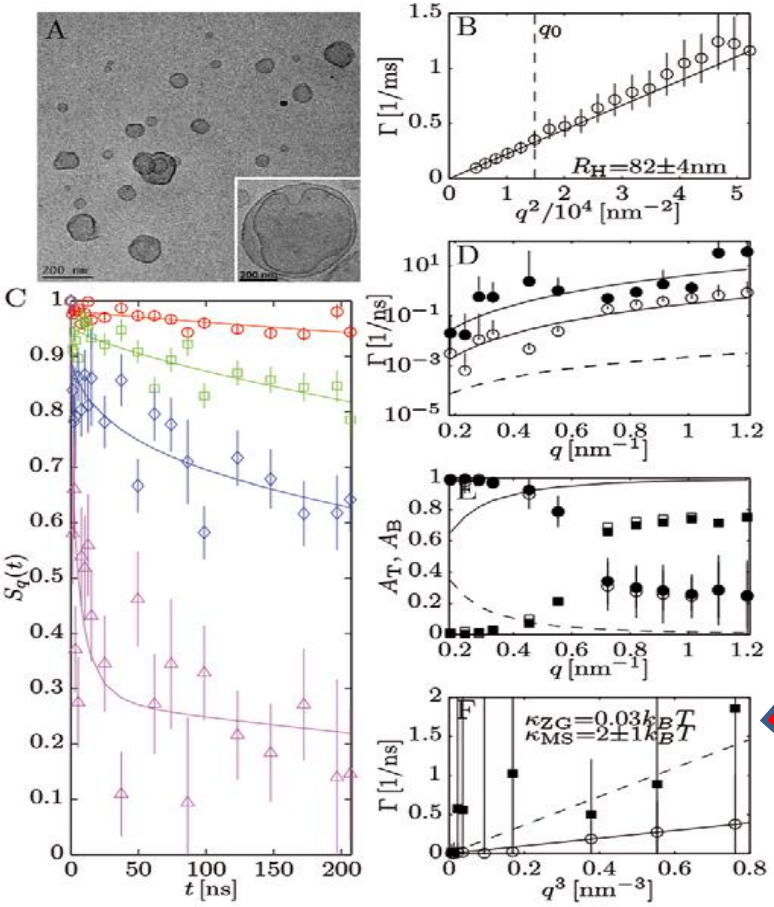

NSE from diluted polymersome dispersions triblock copolymer Pluronics L121

Soluble Pluronic L121 is formed by a **central**, slightly hydrophobic, block of polypropylenoxide (PPO) flanked by two small **lateral chains** of the hydrophilic polyethilenoxide (PEO)

$$\kappa = (2 \pm 1) k_B T$$

Low constant !

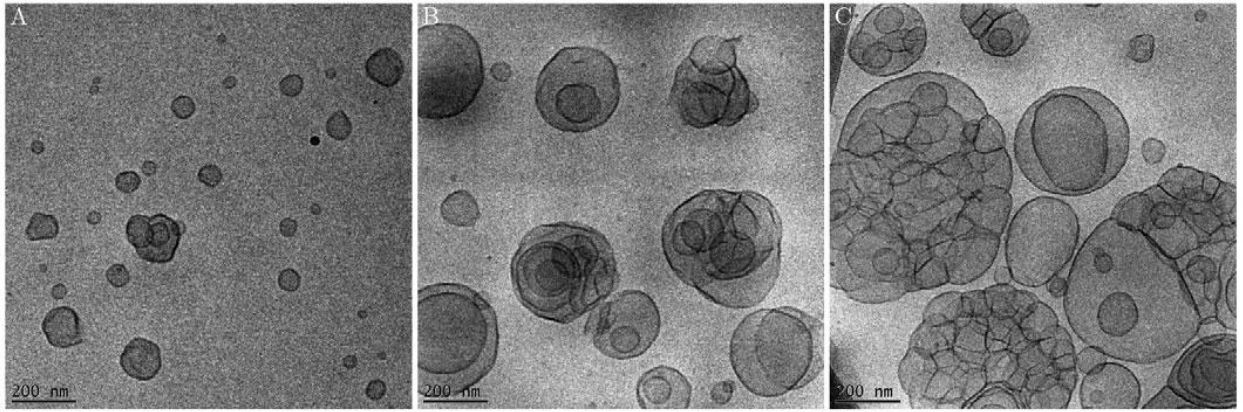

CryoTEM images of samples taken from the same L121 preparation and vitrified **at increasing times** after extrusion (A) immediately after; B) after **1 h**; C) **4 h**. As Vesicles become increasingly agglomerated and fuse together to form ever larger vesicles.

Proteins, NSE? Biologically relevant protein motions

Timescales from femtoseconds to seconds: ***Nanoscale protein dynamics influences***
protein-ligand binding, protein complex formation, and signal transduction

D. J.E. Callaway, B. Farago, and Z. Bu. **Nanoscale protein dynamics: A new frontier for neutron spin echo spectroscopy.** ***//*** Eur. Phys. J. E (2013) **36**: 76

- NSE for long-range protein domain motions
- Nanometer length scales
- Nanosecond to microsecond timescales
- NSE - protein dynamics and functions

How binding signals are propagated in a protein to distal sites?

Selective deuteration can resolve **specific domain dynamics** from the abundant global translational and rotational motions in a protein

Allosteric regulation !

Protein dynamics is essential to **all aspects of protein function**:
protein stability, enzyme catalysis, propagation of allosteric signals
Protein dynamics is hierarchical, occurring on many orders of timescales and multiple lengthscales

Scaffolding protein NHERF1: Modulating the intracellular trafficking and assembly of a number of receptors and ion transport proteins

NHERF1 has **two modular domains**, ***PDZ1, PDZ2***, and a disordered but compact ***C-terminal*** (CT) domain, with three domains connected by unstructured linkers

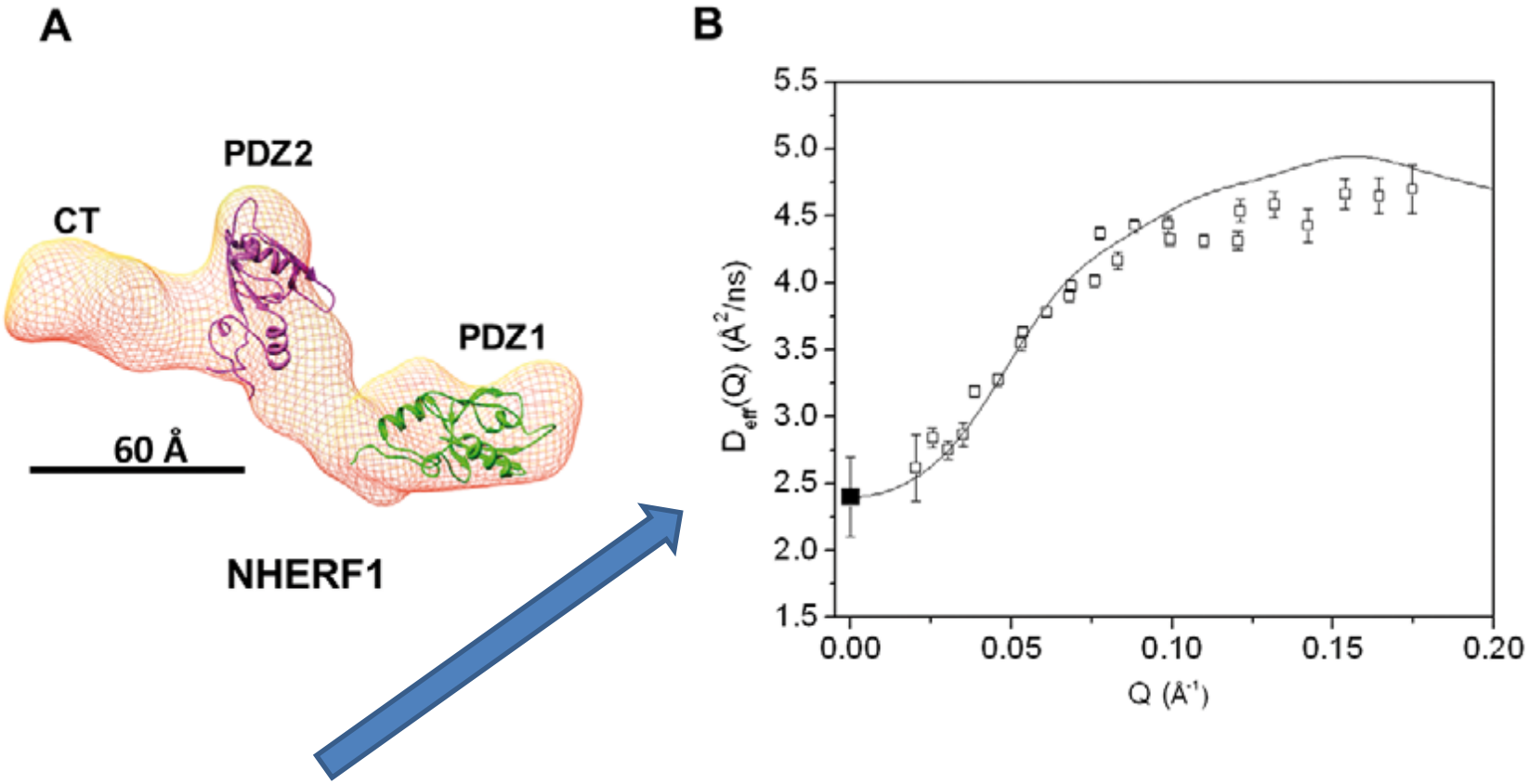

For ***NHERF1 alone in solution***, the calculated **rigid body *D*eff (*Q*)** agrees with the NSE experimental data quite well

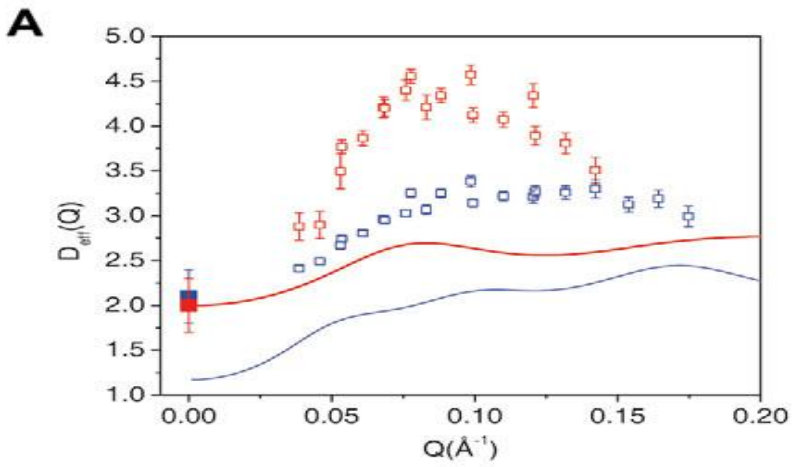

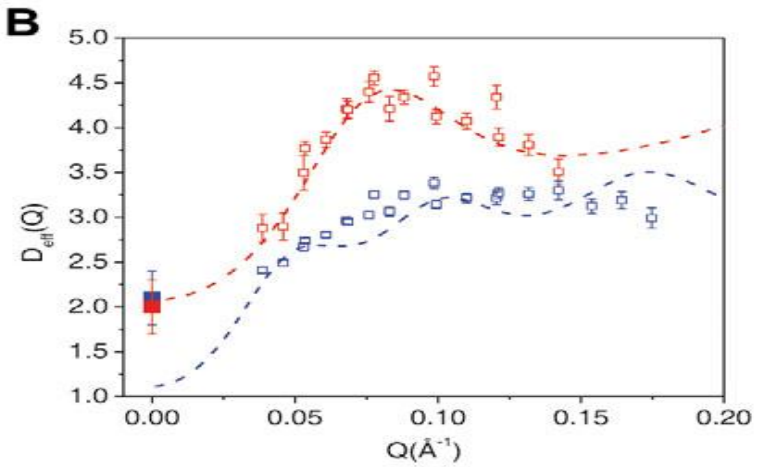

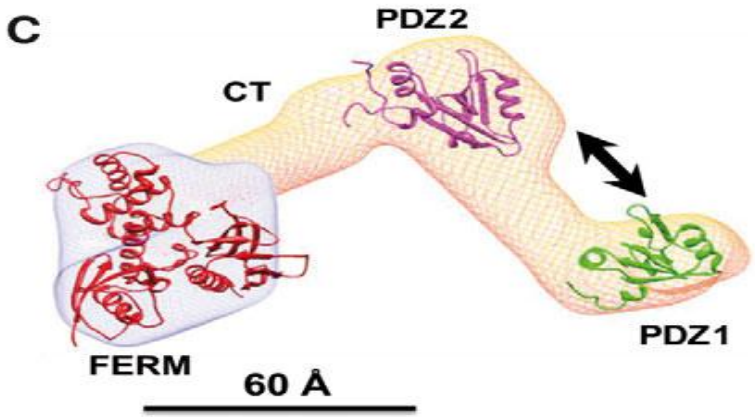

A) Red line - *rigid-body model* - NHERF1·dFERM complex

Blue line - ***rigid-body model*** for NHERF1·**h**FERM complex with FERM hydrogenated

B) ***Deff (Q)*** of ***deuterated complex NHERF1·dFERM***

and hydrogenated complex NHERF1·hFERM, ***interdomain motion*** between PDZ1 and PDZ2

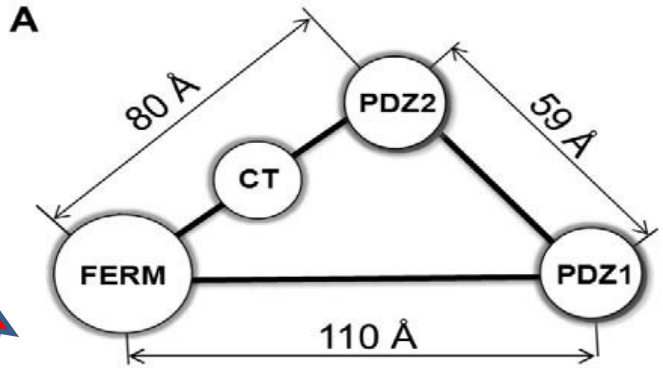

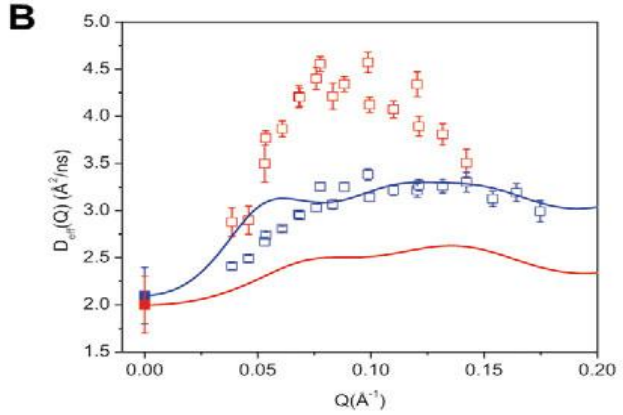

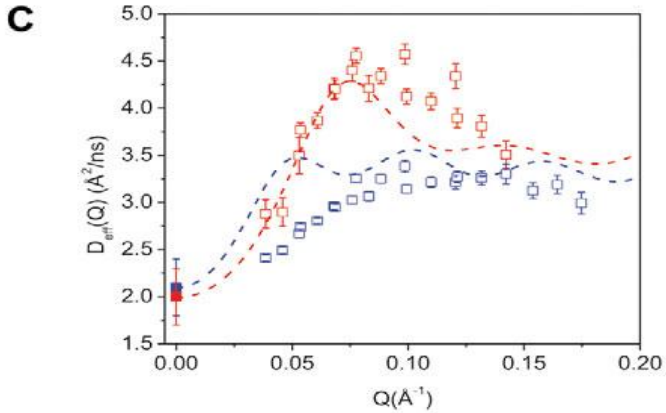

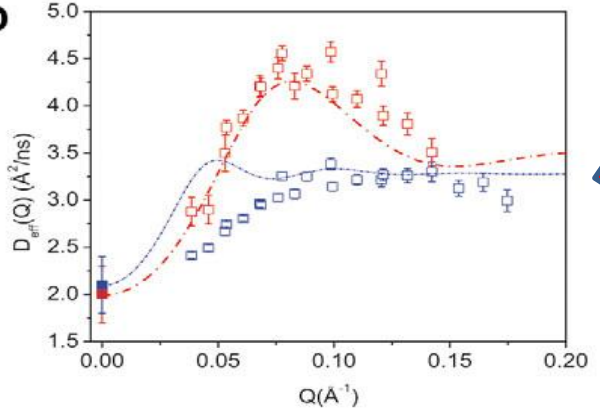

4-point model: A) **NHERF1·FERM complex** with **PDZ1, PDZ2, CT**, and FERM;
B) **4-point rigid-body** calculations for NHERF1·hFERM (**blue**) and for NHERF1·dFERM) (red)
C) ***Inter-domain motion*** between **PDZ1** and **PDZ2** in NHERF1·dFERM (red dash) and NHERF1·hFERM (blue dash)
D) ***Inter-domain motion* between PDZ1 and PDZ2 + finite size form factor of spheres of 20˚A radius for the FERM domain** and for both **PDZ** domains in NHERF1·dFERM (red dash dot line) and in NHERF1·hFERM (**blue dash dot line**).

1. Классическое NSE

   диффузия, релаксация

2. Комбинация NSE + TAS, TOF

   времена жизни возбуждений

3. Четное и нечетное спин-эхо

   ODD + EVEN NSE

   мягкие затухающие моды

   динамика неравновесных систем

Спин-эхо с модуляцией спектра

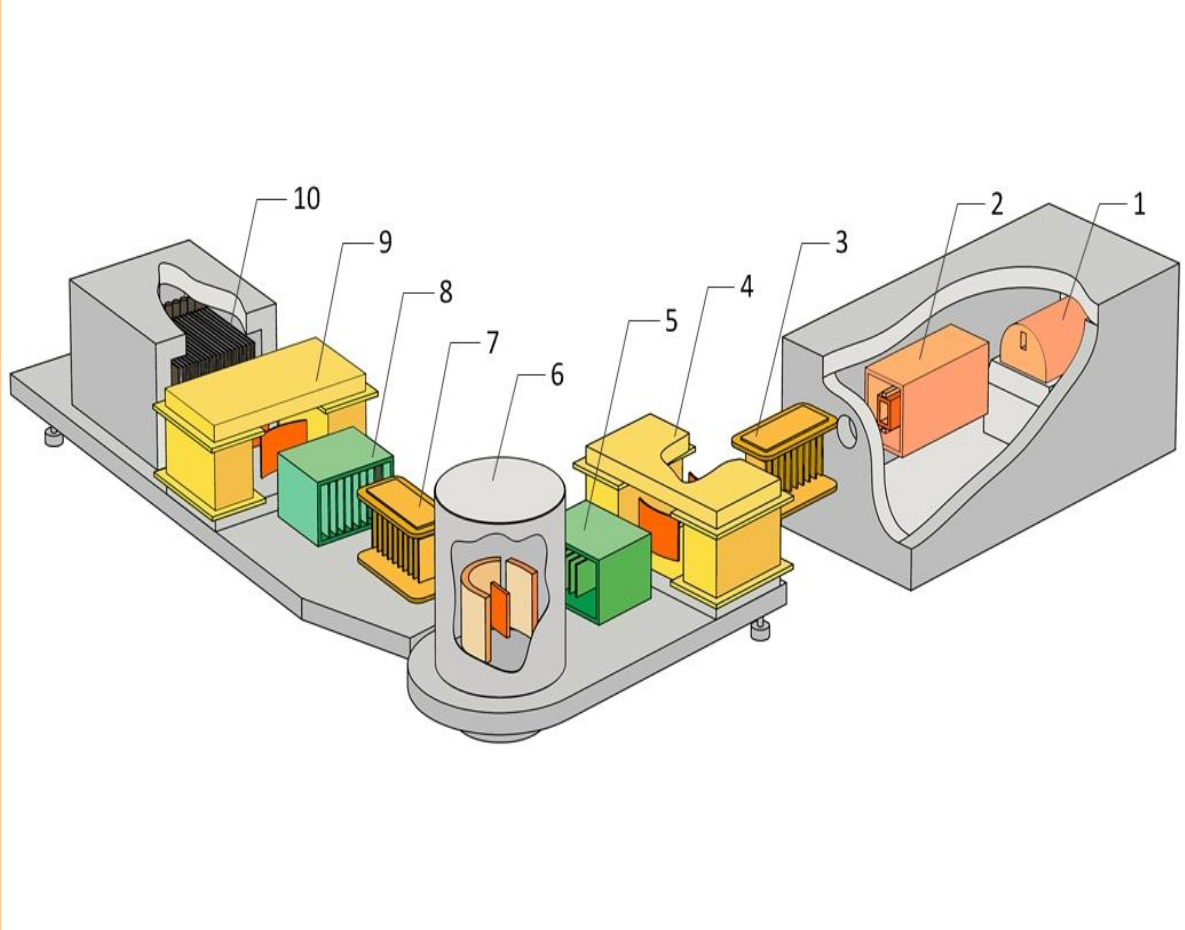

NSE + 3D-polarization Analysis Magnetic, Spin-dependent Incoherent Scattering

*1 – монохроматор, 2 – поляризатор **1**, 3 – радиочастотный флиппер **1**; 4 – магнит прецессии **1**; 5 – поляризатор **2**; 6 – узел образца (внутри - блоки векторного анализа поляризации); 7 – радиочастотный флиппер **2**; 8 – анализатор **1**; 9 – магнит прецессии **2**; 10 – анализатор **2** в сборке с детектором*

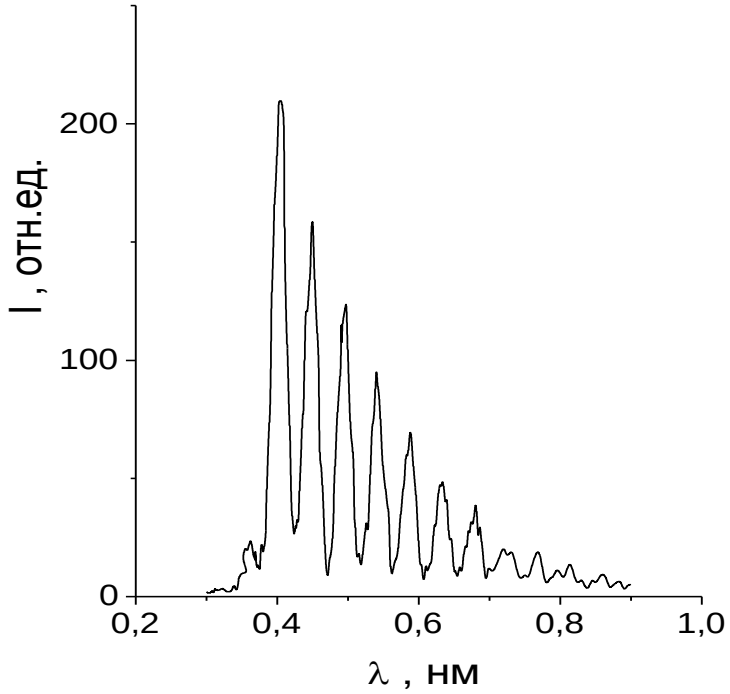

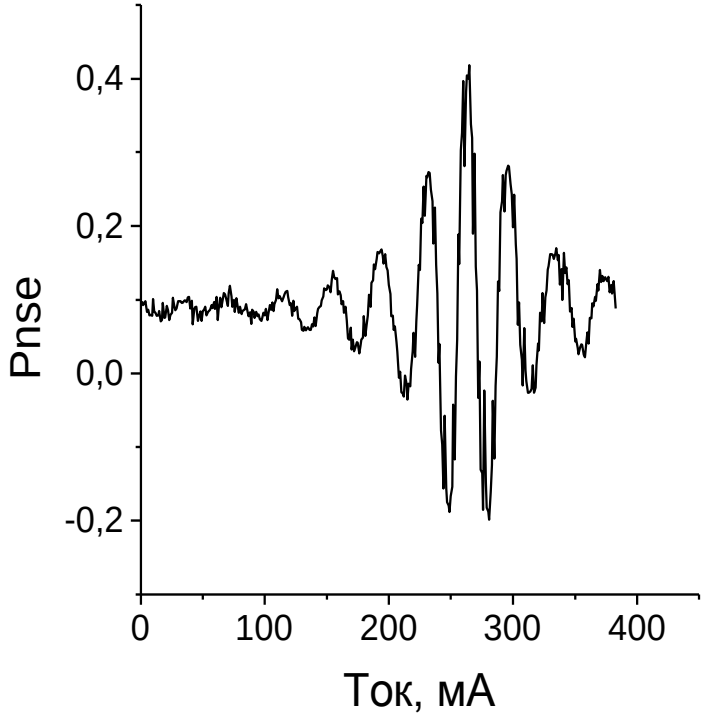

$$\Phi_m(\lambda) = \Phi(\lambda)[1 \pm P_o\cos(2\pi N_1\lambda/\langle\lambda\rangle)]/2$$

N_1 - число прецессий спина нейтрона при $\lambda = \langle\lambda\rangle$, $t = \hbar\pi N/E_o$

$$P_{nse} = (I_{off} - I_{on})/(I_{off} + I_{on}) \approx (1/2)P_o^2 \int\Phi(\lambda)\cos[2\pi(N_2-N_1)\lambda/\langle\lambda\rangle]d\lambda \,/\, \int\Phi(\lambda)d\lambda$$

Концепция нечетного спин-эхо - ODD NSE

$$S(\omega,\mathbf{q}) = S_{odd}(\omega,\mathbf{q})+S_{even}(\omega,\mathbf{q})$$

$$S_{odd}(\mathbf{q},t) \sim \int S(\omega,\mathbf{q})\sin(\omega t)d\omega \quad S_{even}(\mathbf{q},t)\sim\int S(\omega,\mathbf{q})\cos(\omega t)d\omega$$

Сумма нечетной и четной компонент
Преимущества при наличии нечетных сечений
Данные для феррожидкости и раствора полимера

Традиционно NSE-методом получают **COS-Фурье-образ** частотной функции

$$S_{even}(t,\mathbf{q},) \sim \int S(\omega,\mathbf{q})\cos(\omega t)dt$$

Лебедев В.Т. Способ исследования структурно-динамических свойств вещества. Бюллетень изобретений 27.06.2008. № 18. RU 2327975 C1. Патент.

Лебедев В.Т. Принципы обобщенной спин-эхо спектроскопии. // Поверхность. Рентгеновские, синхротронные и нейтронные исследования. 2009. № 6. С. 14-21.

Метод

- В полях $H_{1,2}$, разделеных π-флиппером и ограниченных π/2-фл. поляризация нейтрона $\mathbf{P}_o$ набирает фазу $\varphi=\gamma_L(L_1H_1/v_1-L_2H_2/v_2)$,
- где L_1,L_2 - протяженности полей, γ_L - гиромагнитное отношение, а v_1 и v_2 - скорость нейтрона в $H_{1,2}$ (Рис.1) [2].

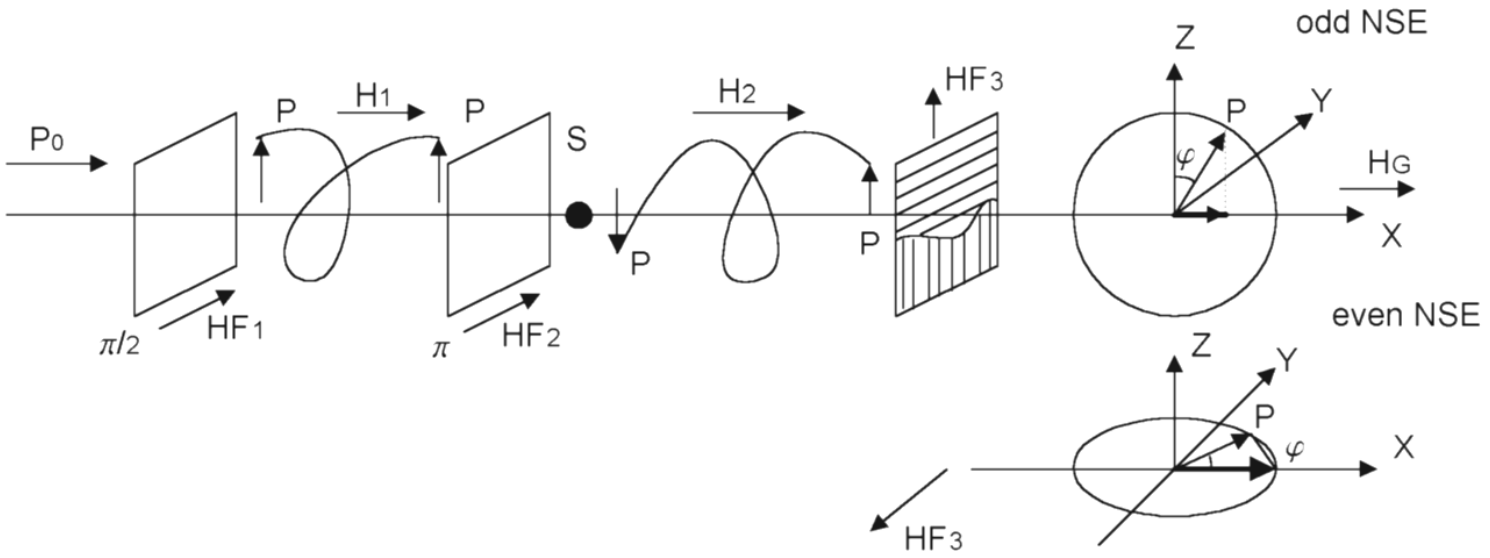

NSE нечетное и четное (верх, низ): эволюция поляризации $P_o \rightarrow P$ при прохождении нейтроном π/2- и π-флипперов (поля $HF_{1,2,3}$, показаны обмотки), полей $H_{1,2}$. Образец S не меняет поляризации

NSE
LLB, Saclay

Tests for
Odd and Even NSE

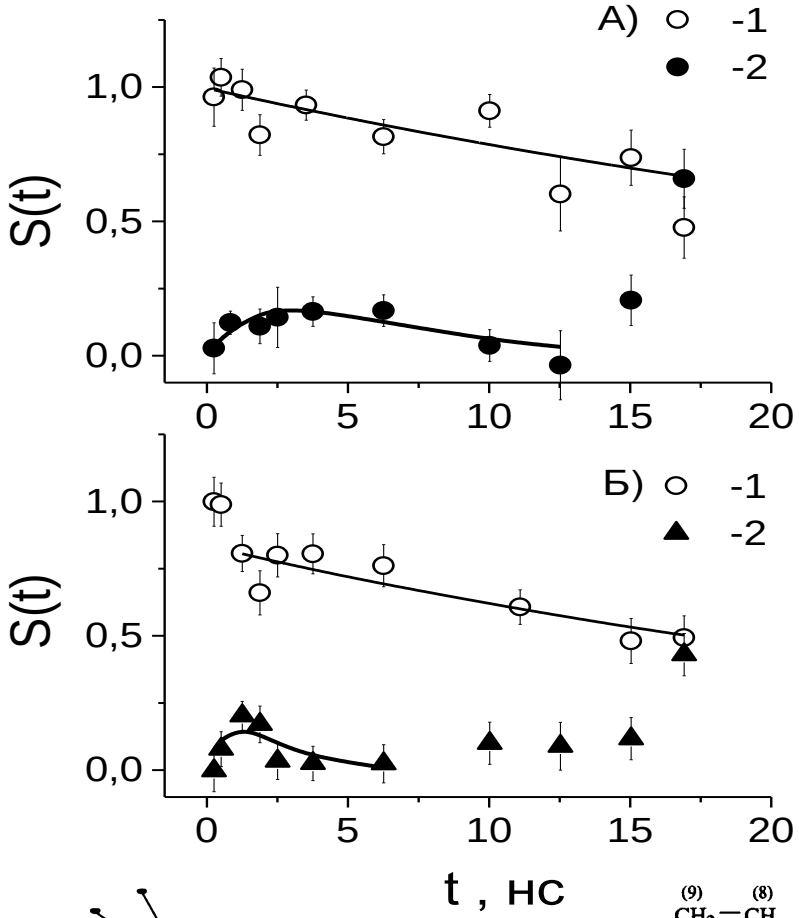

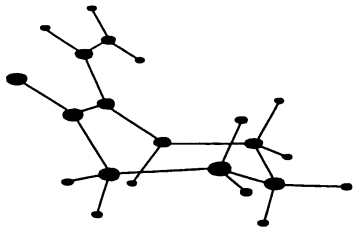

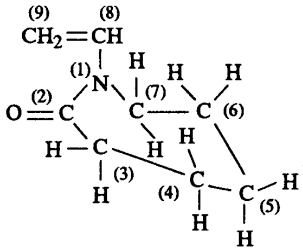

Динамика поливинилкапролактама (ПВКЛ) **четная(1) и нечетная(2)** в D2O при при T_1 = 25.9 °C и T_2 = 26.2 °C (А,Б)

$S_{even}(t) = S_o \cdot \exp(-Dq^2t)$

S_{o1} = 0.995 ±0.049
$D_1 = (2.5\pm0.8)\cdot10^{-6}$ см²/с при $T=T_1$

S_{o2} = 0.836 ±0.041
$D_2=(3.1\pm0.7)\cdot10^{-6}$ см²/с при $T=T_2$

$S_{odd}(t/\tau) \sim t\cdot\exp(-t/\tau)$

$S_{oo1}=0.47\pm0.09$; $\tau_1=3.1\pm0.5$ нс
$S_{oo2}=0.41\pm0.17$; $\tau_2=1.1\pm0.3$ нс

Модель резонанса: $S(\omega,\omega_o) = [(\omega-\omega_o)^2+\delta^2]^{-1}$, ***мягкая мода*** ($\omega_o \sim \delta$)

$S(\omega,\omega_o) \approx (\omega^2+\delta^2)^{-1} - 2\omega_o\omega(\omega^2+\delta^2)^{-2}$

$S_{even} = \exp(-t\delta)$; $-S_{odd} = A\omega\cdot(t\delta)\cdot\exp(-t\delta)$



PIK:
inelastic + SANS
complementary facilities
for nanostructures

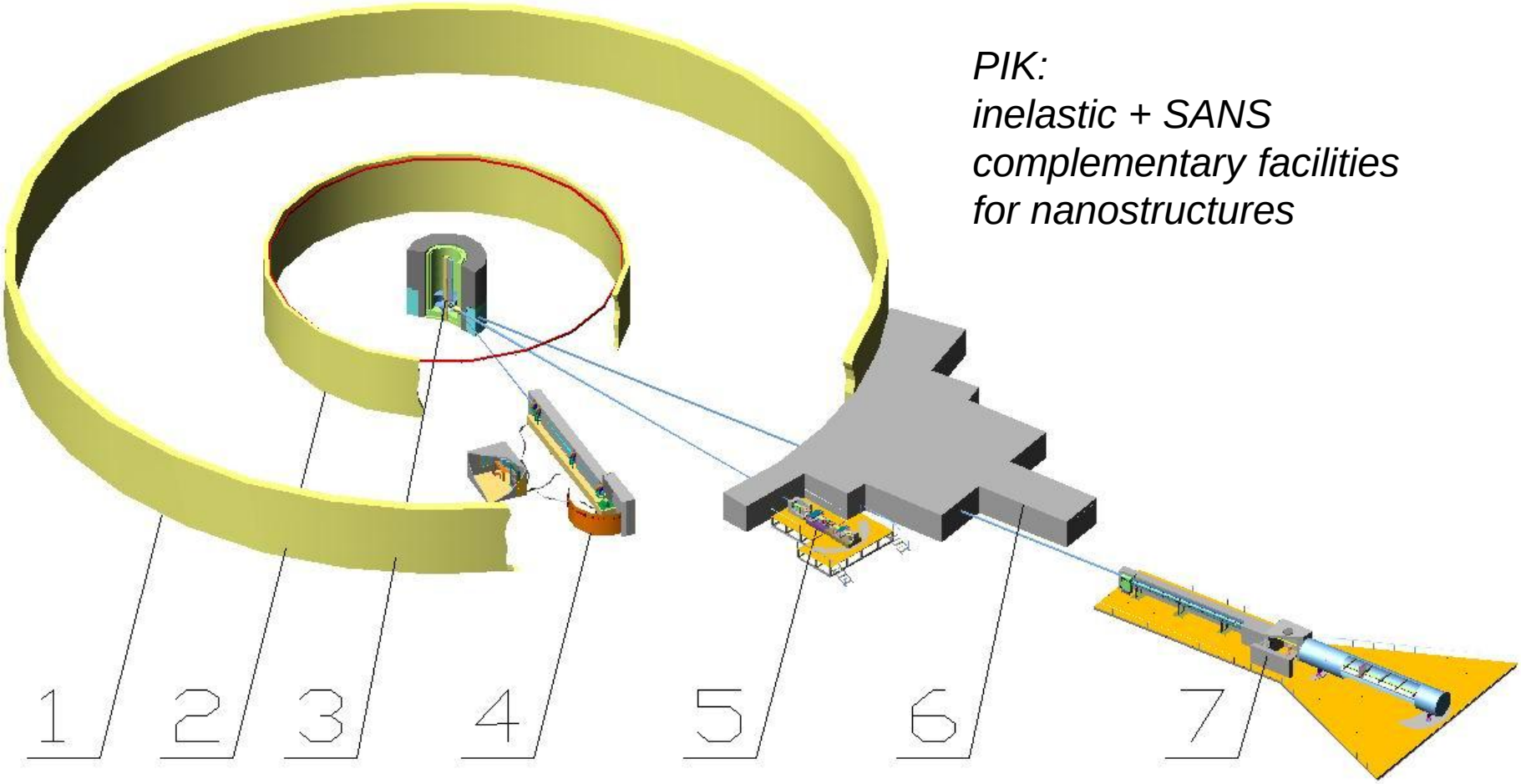

Facilities for structural and dynamical studies: 1,2 - walls of circular hole, 3 - reactor core, 4 - TOF; 5 – NSE, 6 - neutron guides, 7 - "Membrane-3"

Spin-echo using wavelength-spectrum modulation

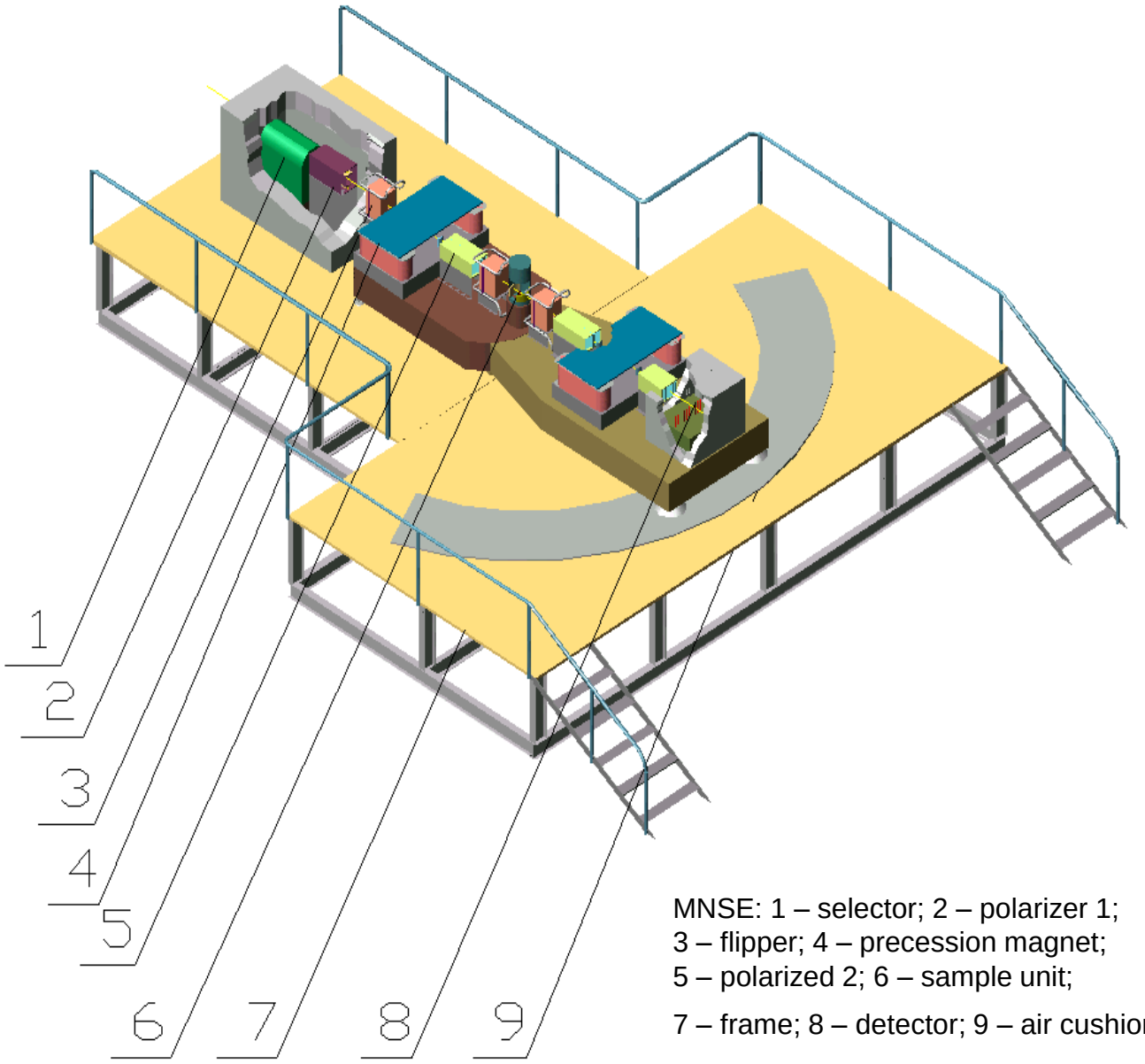

MNSE: 1 – selector; 2 – polarizer 1;
3 – flipper; 4 – precession magnet;
5 – polarized 2; 6 – sample unit;

7 – frame; 8 – detector; 9 – air cushions

Multi-chopper TOF

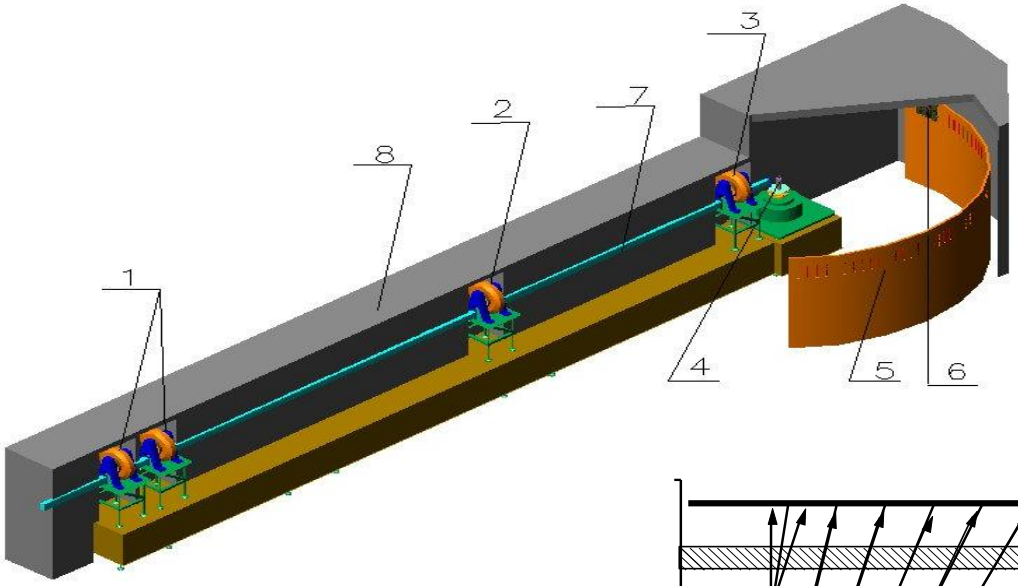

TOF: 1 –double chopper (1,2) and chopper (3) regulating the period between pulses; 2 – zone chopper (4), 3 – chopper (5) defining TOF base; 4 – sample; 5,6 – set of single detectors and 2D-detector; 7 – NG

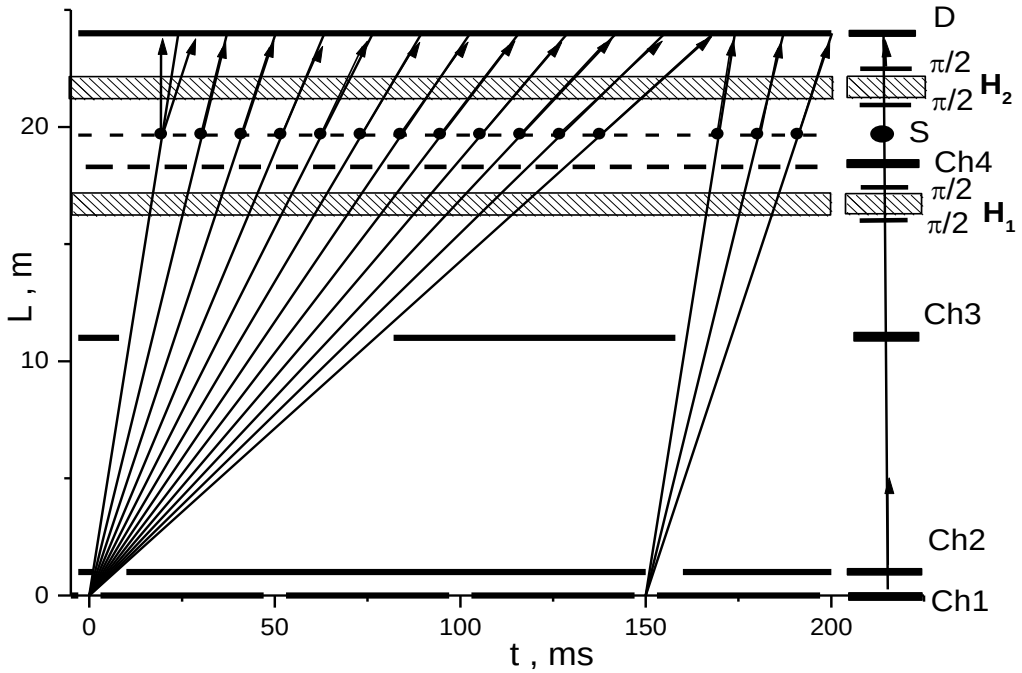

Выводы

1. NSE-technique (cold neutrons) ~ предел по разрешению
2. Развитие комбинированных вариантов
   3D-polarimetry + NSE, TOF + NSE,
   TAS + NSE, SANS + NSE, SESANS + NSE
3. ***Прорыв*** – **Very Cold Neutrons for NSE:**
   biology, catalysis,chemical reactions,
   material science


Спасибо за внимание !